MAPPING EUROPEAN SPRUCE BARK BEETLE (*IPS TYPOGRAPHUS, L.*) INFESTATION USING DESIS IMAGE SPECTROSCOPY AND SENTINEL-2 SATELLITE DATA

RAYMOND KWAME NAGBIJA
JUNE, 2025

SUPERVISORS:
Dr. Roshanak Darvishzadeh
Dr. Haidi Abdullah

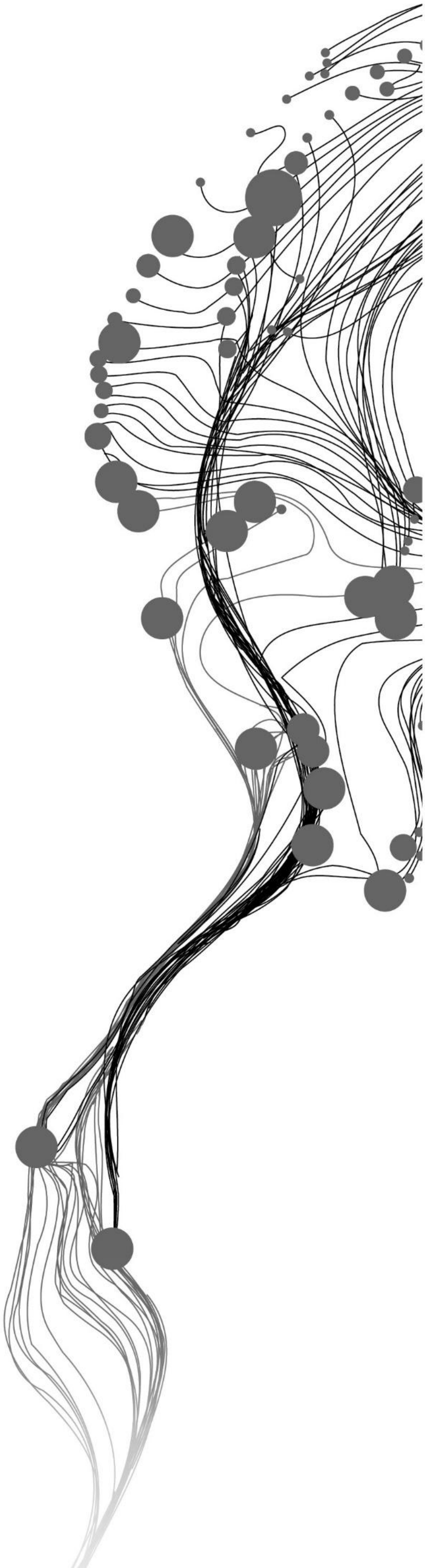

MAPPING EUROPEAN SPRUCE BARK BEETLE (*IPS TYPOGRAPHUS, L.*) INFESTATION USING DESIS IMAGE SPECTROSCOPY AND SENTINEL-2 SATELLITE DATA

RAYMOND KWAME NAGBIJA
Enschede, The Netherlands, JUNE, 2025

Thesis submitted to the Faculty of Geo-Information Science and Earth Observation of the University of Twente in partial fulfilment of the requirements for the degree of Master of Science in Geo-information Science and Earth Observation.
Specialization: Natural Resource Management

SUPERVISORS:
Dr. Roshanak Darvishzadeh
Dr. Haidi Abdullah

THESIS ASSESSMENT BOARD:
Dr. Tiejun Wang (Chair)
Prof. Dr. Marco Heurich (External Examiner, Bavarian Forest National Park)

ABSTRACT

In recent years, forest disturbances worldwide have increased significantly due to factors such as insect outbreaks and wildfires, which are often intensified by prolonged droughts linked to climate change. In Central Europe, the European spruce bark beetle (*Ips typographus* L.) is the primary cause of damage, to temperate forest resulting in millions of tons of dead Norway spruce (*Picea abies*). Traditional detection methods, such as field surveys and aerial photography, are inadequate for large-scale monitoring of such damage and often fail to identify early infestations when intervention is most effective. Satellite remote sensing offers a promising approach for early and large-scale detection of vegetation stress. This study investigated the potential of DLR Earth Sensing Imaging Spectrometer (DESIS) and Sentinel-2 data for assessing bark beetle infestation in Spruce stands in Bavarian Forest National Park (BFNP), Germany. The spectral variability of spruce canopies infested by bark beetles during the green and red attack phases were assessed using Sentinel-2 and DESIS image spectroscopy data and the spectral bands sensitive to early-stage bark beetle infestation (green attack) (i.e., in June)- were identified. Next, the potential of these data for mapping the bark beetle infestation was examined using two Random Forest classification models. To analyze spectral reflectance variations across infestation phases, first the location of healthy and infested canopies was identified using field data and then the reflectance values of these canopies were extracted from Sentinel-2 and DESIS imagery and processed in MATLAB R2024b to generate spectral profiles. The red edge position (REP) was calculated for all infestation phases using the polynomial fitting method. A one-way ANOVA test was applied to all 230 DESIS and 10 Sentinel-2 spectral bands to identify spectral regions/bands sensitive to green attack infestation. Subsequently, two Random Forest models were developed for discriminating against healthy and infested canopies (Model A, used significant bands and vegetation indices, and Model B, which used only the ANOVA-significant bands). Two infestation maps were generated using these models for DESIS and Sentinel-2 datasets.

The results showed that canopies affected by green and red attack exhibited increased reflectance in the visible spectrum and decreased reflectance in the near-infrared region. The analysis demonstrated that REP shifted toward shorter wavelengths as the infestation progressed, indicating stress and chlorophyll degradation. The ANOVA test identified bands in red edge, and near infrared region as significant for detecting bark beetles green attack in both datasets. The Random Forest model results revealed that using reflectance data from significant bands and vegetation indices could allow an enhanced discrimination of healthy and infested canopies during green attack (733 pixels (47%) out of 1,568 pixels in DESIS data, and 1,476 pixels (41%) out of 3,572 pixels in Sentinel-2 data). The findings demonstrate the value of satellite hyperspectral remote sensing data for the early detection of bark beetle infestations, providing a cost-effective tool to enhance forest health monitoring and management during critical early infestation stages.

ACKNOWLEDGEMENTS

First and foremost, I would like to express my deepest gratitude to my thesis supervisors, Dr. Roshanak Darvishzadeh and Dr. Haidi Abdullah, for their invaluable guidance, support, and encouragement throughout this research. Their expertise, insightful feedback, and patient mentoring have been fundamental in shaping this thesis and enriching my learning experience. Their unwavering support has greatly enriched the quality and depth of this thesis. Many thanks to Dr. Tiejun Wang, the chair of my thesis for his guidance, insights, and supportive academic environment.

I wish to extend my heartfelt appreciation to my family for their unconditional love, patience, and continuous encouragement. Their belief in me and their constant support have been a source of strength, motivation, and comfort throughout my academic endeavors.

Special thanks go to my friends, Kiki Winda Veronica, Theo Verheijen, and Elisha Njomaba who have offered moral support, inspiration, and camaraderie during the challenging moments of this journey. Their encouragement and understanding have made this experience more fulfilling and enjoyable. Finally, I acknowledge all those who, directly or indirectly, contributed to the successful completion of this thesis. Without their support, this work would not have been possible.

1. INTRODUCTION

1.1 Background

Forests are under increasing pressure from many factors, including climate change, invasive species and human impact. Of these threats, bark beetle outbreaks stand out as a major problem, with tree mortality and changes to forest structure, biodiversity and ecosystem services (Siegert et al., 2024). The European spruce bark beetle (*Ips typographus*) is a major pest affecting coniferous forests throughout Europe, with outbreaks becoming significantly more frequent and severe in recent decades (Abdullah et al., 2019; Netherer & Schopf, 2010). This is directly linked to climate change, with warmer temperatures and decrease precipitation patterns creating conditions for beetle growth and weakening of host tree defenses (Seidl et al., 2016; Hlásny et al., 2021). These climate changes make forests more vulnerable and more prone to big dieback events with far reaching ecological and economic consequences.

The impacts of bark beetle outbreaks go far beyond local ecological damage. Forest dieback leads to significant carbon loss, accelerating climate change and disrupting global carbon cycles (Luyssaert et al, 2008). Forest loss also reduces biodiversity, changes hydrological processes and diminishes the provision of ecosystem services like timber, recreation and soil protection (Bonan, 2008). On the other hand, the economic consequences are huge for forestry, tourism and local communities dependent on forest resources (Mayer et al., 2010). The Bavarian Forest National Park (BFNP) in Germany is a prime example of the challenges posed by bark beetle outbreaks since 1980s, (Heurich et al, 2009). This protected area, known for its biodiversity and ecological integrity, has been heavily damaged by *Ips typographus* infestations (Abdullah et al., 2019). Its ecological importance and status as a major eco-tourism destination make it imperative to have innovative and cost-effective bark beetle management.

To develop targeted interventions, the lifecycle of *Ips typographus* needs to be understood. The development of beetles goes through four stages: egg, larva, pupa and adult (Vege & Hofstetter, 2015). Adult beetles start by boring into the bark of host trees and creating galleries for egg laying. The hatching larvae feed on the phloem, the tree's vital nutrient-transporting tissue, disrupting its physiological functions and ultimately killing the tree. This feeding weakens the tree's defences, making it susceptible to secondary infections and accelerating the decline. The rapid lifecycle of *Ips typographus* and its ability to infest multiple trees can lead to exponential population growth and rapid spread of outbreaks (Marx, 2010). Which needs to be understood before effective management plans can be implemented. Bark beetles go through three visual phases: green, red and grey (Kautz et al., 2023). The green phase, or green attack, is the initial stage of infestation and is characterised by subtle physiological changes in the tree that are not visible. This makes early detection very difficult, as traditional monitoring methods do not notice infestations at this stage. The red phase, or red attack, is the active decline of the tree, with needles turning reddish brown as the tree dies. The grey phase, or grey attack, is when the tree is dead, and the remaining deadwood stands are of no nutritional value to the beetles. Intervention is most effective during the green phase when beetle populations are small and can be contained. But this phase is cryptic and requires advanced detection methods to detect and monitor the spread.

Traditional methods for monitoring bark beetle infestations, such as ground surveys, aerial photography and manual inspections, have inherent limitations (Fahse & Heurich, 2011). While these methods can work at small scales, they are laborious, expensive and often not practical for large scale and remote forested areas. Aerial photography and visual inspections, for example, can only detect infestations when symptoms are visible, that is, the red and grey phase, when the damage is already done. These limitations highlight the need for more efficient and proactive monitoring approaches. In this regard, remote sensing technologies have become powerful tools for large-scale forest health monitoring, offering repeated data acquisition over large areas, reduced long-term costs and the ability to detect subtle changes in vegetation condition (Coops et al., 2006).

Satellite multispectral sensors like those on Landsat and Sentinel-2 satellites provide valuable information on vegetation health through indices like the Normalised Difference Vegetation Index (NDVI) and red-edge indices (Lausch et al., 2013; Abdullah et al., 2018). These indices are sensitive to changes in chlorophyll content, leaf area index and other biophysical parameters and give a general indication of forest health. However multispectral data often lacks the spectral resolution to detect the subtle physiological changes associated with early-stage bark beetle infestations.

Hence, there is a need for hyperspectral imaging; hyperspectral data consists of more than hundreds of narrow spectral bands from visible to shortwave infrared 400-2500nm, which enables much more detailed information about vegetation spectral signatures, with a high spectral resolution that can detect minor variations with external reflectance across the electromagnetic spectrum, thus providing information on the physiological condition of the plant, (Ustin & Gamon, 2010). Hyperspectral data can also highlight the alterations in chlorophyll content, water content, and other biochemical components that may indicate stress, even before symptoms occur (Zarco-Tejada et al., 2018). One of the spectral regions sensitive to chlorophyll concentration changes and is regarded as a key indicator of plant stress, is the red-edge region (680-740 nm), which is situated between the red and near-infrared regions of the electromagnetic spectrum, (Somers & Asner, 2013; Hlásny et al., 2013). An increase in red-edge reflectance or a shift in its position serves as an early indicator of bark beetle infestation. Specifically, a shift toward shorter wavelengths (known as a blueshift) often signals vegetation stress, which can reflect the initial stages of bark beetle disturbance, (Velichkova & Krezhova, 2019).

Previous research has demonstrated that hyperspectral remote sensing holds strong potential for the early detection of bark beetle infestations, (Lausch et al., 2013; Näsi et al., 2015; Hellwig et at., 2021b, Marvasti-Zadeh et al., 2023; Darvishzadeh et al., 2020). Hyperspectral imagery captured from Fabry Pérot Interferometer (FPI) camera mounted on a UAV (unmanned aerial vehicle) has been utilized to detect infested trees from healthy trees, determine critical spectral features linked to various infestation stages, and map the spatial distribution of outbreaks (Näsi et al., 2015). Lausch et al. (2013) used vegetation indices from HyMAP airborne hyperspectral data to predict future bark beetle outbreaks with reference to spruce forest vitality at different scales. However, while airborne hyperspectral sensors provide high spectral resolution, their application is often constrained by limited spatial coverage and the logistical challenges of frequent data acquisition. To overcome these limitations, satellite-based hyperspectral imaging emerges as a promising alternative for monitoring large, forested areas more efficiently and consistently. One such sensor, the DLR Earth Sensing Imaging Spectrometer (DESIS) aboard the International Space Station (ISS), which is the focus of this research, provides hyperspectral data with a moderate spatial resolution of 30m and a high spectral resolution up to 235 spectral bands spanning across the visible and near-infrared(NIR) region 400-1000nm, pave a way toward new capabilities to monitor forest health at regional scales.

Effectively utilizing this wealth of spectral information requires advanced data analysis techniques. Hyperspectral data processing and classification techniques are complex, given the dimensionality of the data, which needs appropriate processing. In recent years, Random Forest (RF) and Support Vector Machine (SVM) have gained great popularity for the classification of complex and high-dimensional datasets like hyperspectral images (Breiman, 2001). RF is an ensemble learning method that combines the predictions of multiple decision trees, providing robust and accurate classification results (Krstajic et al., 2014). RF also offers the advantage of feature importance analysis, allowing for the identification of the most relevant spectral bands for discriminating between different classes, for example, in the case of infested and healthy spruce stands. This information can be used to optimize classification models and improve the understanding of the spectral changes associated with bark beetle infestation.

This research aims to address the critical need for early detection of bark beetle infestations with satellite-based hyperspectral data by leveraging the unique capabilities of DESIS image spectroscopy and multispectral imaging from Sentinel-2 satellite. The study will focus on the following key objectives: (i) to examine the spectral variability of bark beetles infested canopies across different infestation phases (from green to red phase), (ii) to identify key spectral bands/regions in Sentinel 2 multispectral data and DESIS image spectroscopy data that are most informative for detecting and mapping early-stage bark beetle infestations (green phase). By focusing on early detection, this research seeks to provide forest managers with cheap, timely and actionable data for implementing effective control measures and mitigating the impacts of bark beetle outbreaks.

1.2 Problem Statement

Bark beetle infestations, particularly those caused by the European spruce bark beetle (*Ips typographus*), have emerged as a significant ecological and economic threat to European coniferous forests. Climate change-related factors, such as rising temperatures and prolonged droughts, have increased both the frequency and severity of these infestations, leading to widespread tree mortality and forest degradation. Such outbreaks jeopardize biodiversity, disrupt carbon sequestration processes, and pose challenges to forestry and industries dependent on eco-tourism. For example, the Bavarian Forest National Park (BFNP) provides substantial economic benefits to the governments of Germany and the Czech Republic. According to Stemberk, (2020) , BFNP, gross turnover was € 52.4 million with a calculated annual attendance of 1,361,367 peoples in 2020. Additionally, the tourism industry supports employment equivalent to 456 full-time jobs, while the park's administrative department provides about 200 full-time positions (Mayer et al., 2010). This level of development distinguishes BFNP from other national parks in the country.

While BFNP attracts visitors worldwide due to its dynamic and breathtaking landscapes, recent increases in bark beetle activity threaten these natural assets. The landscapes are at risk of collapse, underscoring the urgent need for smart and innovative management strategies to control infestations. Traditional detection methods, such as field surveys and aerial photography, are inadequate for large-scale monitoring and often fail to identify infestations in their early stages, when intervention is most effective in preventing further spread.

Remote sensing technologies, in particular hyperspectral data, offer a promising solution for large-scale forest monitoring. Multispectral and hyperspectral sensors provide valuable information on vegetation health. However, multispectral data lack the spectral resolution necessary to detect subtle physiological changes characteristic of early-stage infestations, particularly during the "green attack" phase when visual symptoms are absent. Hyperspectral remote sensing, especially via satellite platforms like the DESIS, overcomes these limitations by providing high spectral resolution up to 235 spectral band which span across visible to near infrared region capable of detecting early signs of vegetation stress.

Despite this potential, research on using DESIS data to map bark beetle infestations at various stages at the canopy level remains limited, particularly in European forests suffering significant ecological damage. A major challenge lies in identifying the most informative spectral bands to differentiate between healthy and infested spruce stands and developing effective classification strategies for early detection.

Without accurate and timely mapping of infestation hotspots, forest management tends to be reactive rather than proactive, increasing the risk of extensive forest loss. This research aims to address this acknowledge gap by evaluating the potential of DESIS image spectroscopy data and Sentinel-2 multispectral data to detect and map bark beetle infestations, specifically the green attack phase, at the canopy level in the Bavarian Forest National Park.

1.3 Research Objectives , Questions and Hypothesis

Given the identified research gaps, there is a clear opportunity to advance the understanding of how DESIS image spectroscopy data can be used to detect and map bark beetle infestations at the canopy level in the Bavarian Forest National Park (BFNP). The primary objective of this study is to detect and map green-stage bark beetle infestations at the canopy level using DESIS image spectroscopy data and Sentinel-2. To achieve this, the study is organised around the following specific sub-objectives and research questions:

I. To assess the spectral variability of healthy and infested canopies (across different infestation phases) using Sentinel-2 and DESIS image spectroscopy data.
   - How do the spectral characteristics of healthy and infested canopies (vary at different infestation phases) ?
   - How do the red edge position (REP) (vary across different infestation phases)?

II. To examine the potential of Sentinel-2 and DESIS image spectroscopy data to map early-stage bark beetle infestation (green attack) using RF classification
   - Which spectral bands derived from Sentinel-2 and DESIS imagery are most important for successfully mapping early-stage bark beetle infestation (green attack)?

1.4 Research Hypothesis

- ✓ The spectral characteristics of spruce canopies differ significantly between healthy trees and those at different phases of bark beetle infestation, particularly in the red edge (680nm - 750nm) and NIR (750nm-1000nm) regions
- ✓ The REP of infested canopies shifts toward shorter wavelengths during the green and red attack stages of bark beetle infestation, whereas in healthy (uninfected) trees, the red edge remains at longer wavelengths
- ✓ Spectral bands within the red edge (680nm-750nm) and NIR (750-1000nm) are most important for mapping early-stage bark beetles infestation (green attack)

2 METHODOLOGY

This chapter provides a detailed description of the study area and the workflow of this research, including preprocessing of the satellite data, extraction of spectral reflectance for all phases of bark beetles infestation, calculating of red-edge position (REP), identifying significant spectral bands to map bark beetles green attack and mapping bark beetles green attack using RF, as show in (Figure 1)

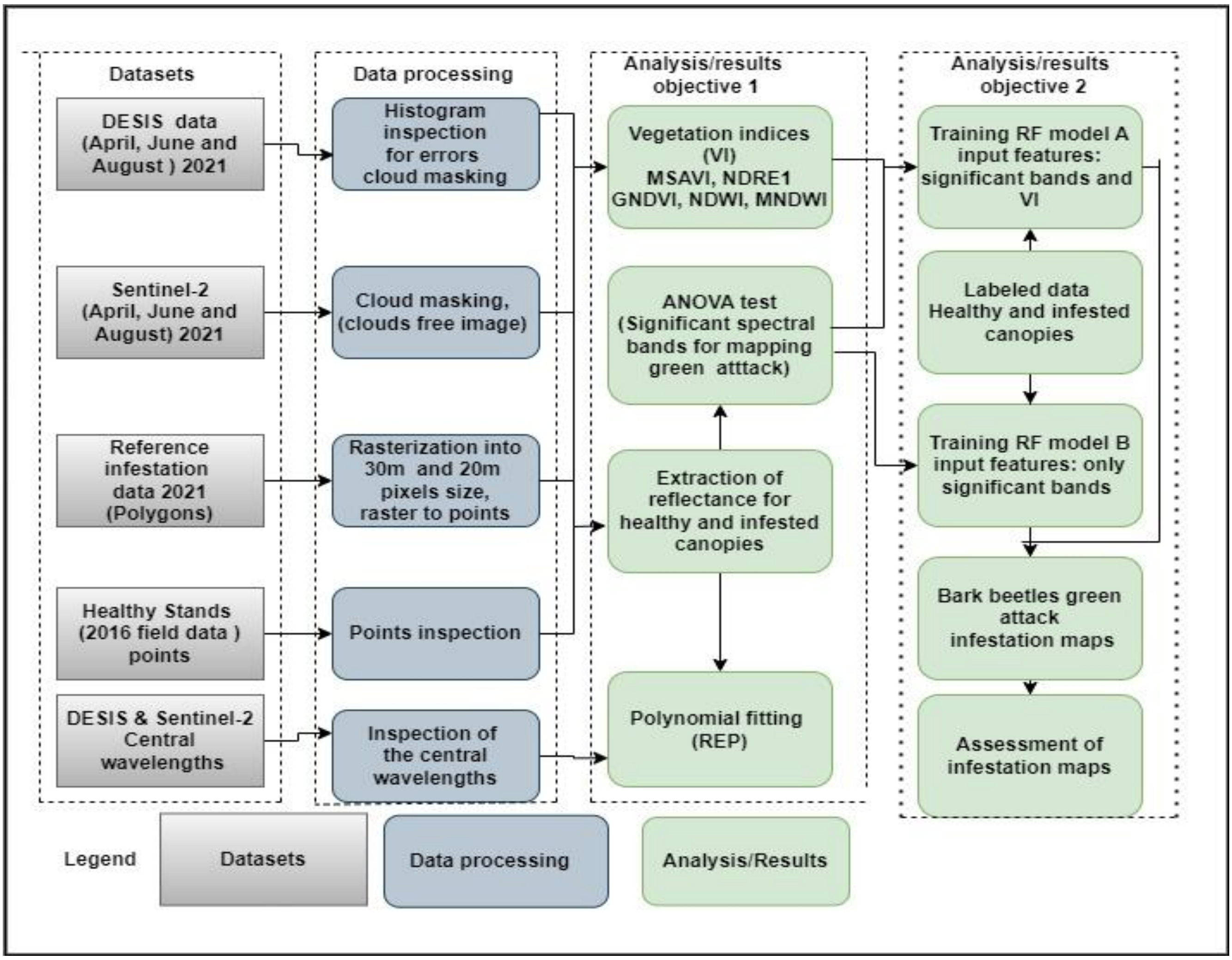

Figure 1: Research methodology flowchart

2.1 Study Area

The Bavarian Forest National Park (BFNP) situated across the Czech Republic's border in southeast Germany. It has a rough extent of 48°55' N to 49°15' in latitude and 13°10' E to 13°45' in longitude, covering an approximate area of 24,000 hectares as shown (Figure 2). The area is characterized by forested mountainous terrain, rising 600-1450 m. It comprised of dense coniferous forests with higher elevation, above 1100m, dominated by Norway spruce (Picea abies) very sensitive to the bark beetle (Biedermann et al., 2019). The choice of the Bavarian Forest as the study area is motivated by several factors directly related to the research problem on mapping bark beetle infestations. The area has a history of severe bark beetle outbreaks, specifically with the European spruce bark beetle (*Ips typographus*), (Heurich et al.,2010). This insect outbreaks have caused severe ecological and economic damage, for example, far-reaching tree mortality, and pose a most serious threat to forest health and biodiversity (Seidl et al., 2016). The persistent bark beetle infestations in the BFNP make it an ideal natural laboratory for testing the capabilities of new imaging spectroscopy satellite data, such as those provided by the DESIS, PRISMA and EnMAP satellites. The BFNP is part of a larger transboundary conservation area including the Šumava National Park in the Czech Republic. It represents an extremely valuable area for nature conservation, with its large old-growth forests and a variety of habitats that have been under rapidly growing pressure due to climate change-induced disturbance, such as outbreaks of bark beetles (Heurich et al.,2010).

The BFNP provides significant economic benefits to the governments of both Germany and the Czech Republic. According to Stemberk, (2020) , BFNP, gross turnover was € 52.4 million with a calculated annual attendance of 1,361,367 peoples in 2020. Furthermore, the tourism industry generates employment equivalent to 456 full-time jobs, while the park's administrative department offers around 200 full-time positions (Mayer et al., 2010). This development distinguishes BFNP from other national parks in the country. The park attracts tourists due to its dynamic ecosystems and breathtaking landscapes.

.

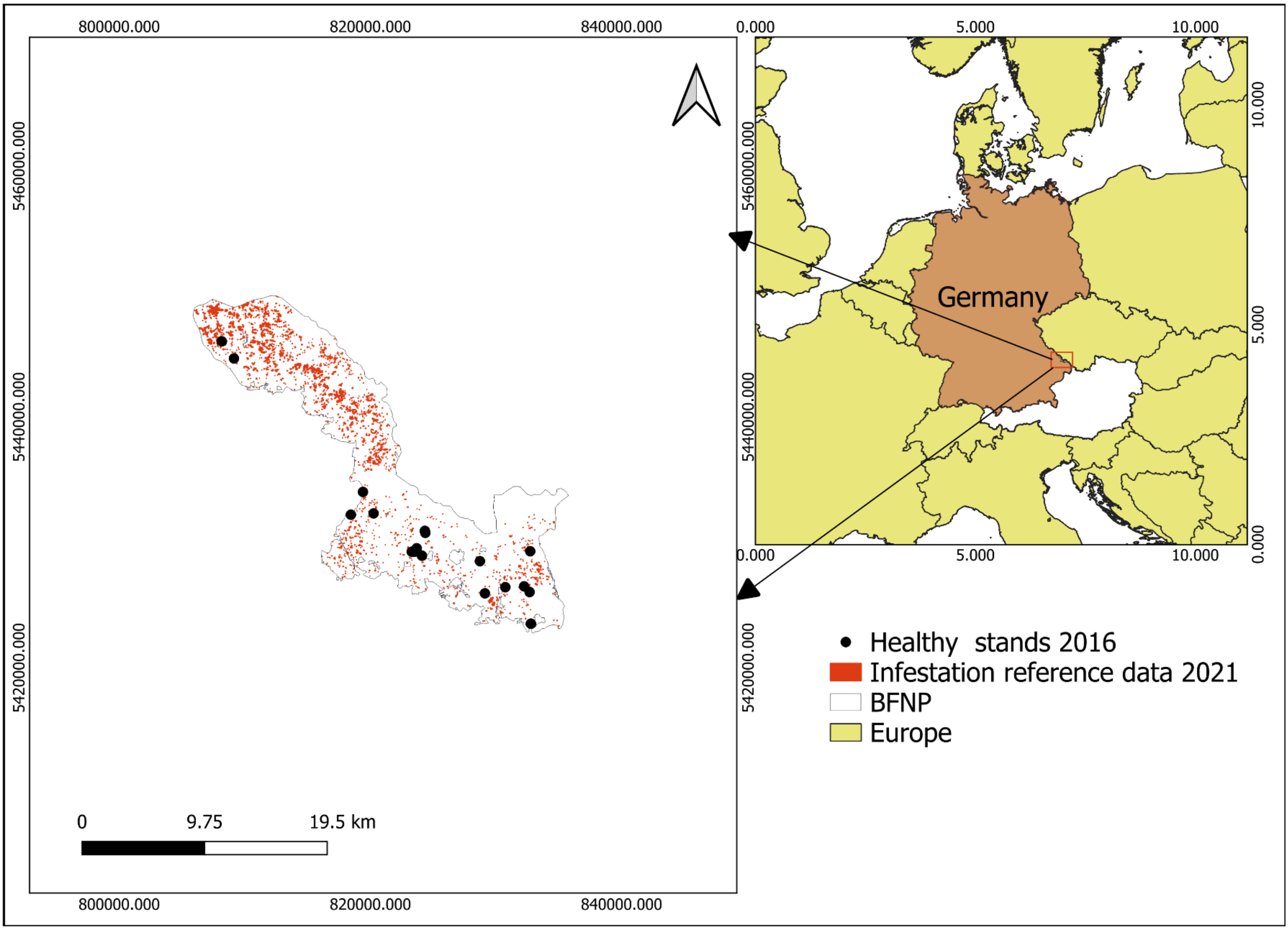

Figure 2: Study Area, Bavaria Forest National Park, the location of bark beetles infestation (2021), and healthy stands (2016).

2.2 Data

To achieve the objectives of this research, we used multispectral imagery from Sentinel-2, imaging spectroscopy data from DESIS, reference data on bark beetle infestations and healthy spruce stands, as well as land use/land cover information. These datasets supported the assessment of spectral variability across different infestation phases and enabled the mapping of early-stage infestations within the study area. Both raster and vector datasets were utilized, as detailed in Table 1.

Table 1: Summary of the datasets used in this study

Datasets	Source	Purpose
BFNP boundaries	BFNP	Used as the National Park boundary
DESIS	DLR (German Aerospace Center)	High spectral resolution image spectroscopy data to identify subtle changes in vegetation due to bark beetles (400nm-1000nm)
Location of the bark beetles' infestation	BFNP	Contain the location of the bark beetles' infestation in the study area
Location of healthy spruce stands	Field campaign 2016	Contain the location of healthy spruce canopies in the study area
Land use Land cover.	BFNP	This data contains different land use and land cover of the study area, including different forest species. Used to mask out non spruce forest before running the RF model
Sentinel 2	Copernicus hub	A moderate spectral resolution is used to identify subtle stress due to bark beetles (443nm - 2190nm)
Sentinel-2 and DESIS Central wavelengths	Copernicus hub and DLR	Contains the wavelengths at which each band are measure. Used for plotting spectral curves and calculation of REP

2.2.1 DESIS image spectroscopy

The DESIS L2A product, acquired on April 10, 2021, June 17, 2021, and August 11, 2021, was used in this study, obtained through special access granted by DLR. These dates correspond to the different phases of bark beetle infestation analysed in this research: prior infestation (April), the green attack (June), and the red attack (August), respectively. Since the DESIS L2A product is already atmospherically and geometrically corrected, no further preprocessing was required for the data. However, the data was visually inspected using the histogram tool in ENVI 6.1 to ensure that all bands and spectral regions were free of potential issues. After the inspection, the wavelength range between 402 and 411.2 nm was found to be irrelevant for this study, so these wavelengths were removed from further analysis, in all a total of 230 spectra bands were remaining for the analysis.

Table 2: Sensor characteristics of DESIS image spectroscopy data based on the HDR file

Spectral Regions	Wavelength ranges (nm)	Spatial resolution (m)	Number of bands
Blue	401.9 - 491.4	30	38

Green	493.8 - 560.5	30	27
Red	563.0 - 678.3	30	45
Red edge	680.8 – 749.7	30	28
Near Infrared	752.2 - 999.50	30	97

2.2.2 Sentinel-2 data.

Sentinel-2 images acquired on 15th April 2021, 25th June2021, and 15th August 2021 from the Copernicus hub were used in this study. These dates correspond to the stages of bark beetle infestation examined in this study: prior infestation (April), green attack (June), and red attack (August). These dates were selected to closely match the dates when DESIS hyperspectral data were obtained (see Section 4.2.1), ensuring the comparability of the two datasets. cloud masking was applied to the images before downloading. The images were acquired from Copernicus hub, downloaded through Google Earth Engine (GEE) and later exported to GIS software for further analysis. Sentinel-2 has bands with spatial resolutions of 10m, 20m and 60m. In this study, Band 1,9, and 10 (443nm, 940nm and 1375nm respectively) were excluded from further analysis, and the remaining 10 bands (Table 3) were resampled into pixel size of 20m.

Table 3: Sensor Characteristics of Sentinal-2 According to ESA (European Space Agency).

Bands	Spectral regions	Wavelengths (nm)	Spatial resolution (m)	Resampled (m)
B2	Blue	490	10	From 10 to 20
B3	Green	560	10	From 10 to 20
B4	Red	665	10	From 10 to 20
B5	Red edge 1	705	20	Default
B6	Red edge 2	740	20	Default
B7	Red edge 3	783	20	Default
B8	Near Infrared (NIR)	842	10	From 10 to 20
B8A	Narrow Infrared (NIR)	865	20	Default
B11	Shortwave Infrared (SWIR)1	1610	20	Default
B12	Shortwave Infrared (SWIR)2	2190	20	Default

2.2.3 Reference Data for Healthy and Infested Norway Spruce Stands

The BFNP authorities have systematically recorded bark beetle infestation incidences using flight campaigns employing airborne colour-infrared (CIR) imaging, collecting data (NIR and VIS) regions with a spatial resolution of 0.1m (Abdullah, 2018a). Two flight campaigns are conducted annually: one in June/July to capture data on recently fallen deadwood from the previous year's infestation, and another in September/October to evaluate tree mortality during the current year.

Each campaign generates 2,528 CIR aerial images at a 20cm resolution, producing a dataset of approximately 147 GB.

Prior to year 2000, these images were manually processed and later digitized. From 2001 onwards, advancements in photogrammetry enabled the use of 3D analysis and software tools like ERDAS StereoAnalyst to compare annual changes in deadwood patches (Lausch et al., 2013a). Mapping efforts focus on areas with five or more dead trees per plot. The processed data is vectorized, containing detailed spatial information on the locations of infested spruce trees.

For this study, the vector-based (polygon) infestation data for 2021 were obtained from BFNP, aligning with the DESIS and Sentinel-2 data captured in the same year. This dataset was used as reference data to identify the locations of infested in forest patches for the extraction of their spectral reflectance. The extracted reflectance profiles of infested canopies were compared with those of healthy spruce trees for further analysis.

In the summer of 2016, a total of 41 healthy Norway spruce plots, each measuring 30 × 30 meters, were identified based on a prior field survey conducted in 2015, which included repeated in-situ assessments of foliar properties across selected tree stands (Abdullah et al., 2018a). These plots were chosen to represent areas free from bark beetle infestation, with careful consideration of forest heterogeneity, including variations in species composition, tree age, and stand density. To ensure data reliability, the plots were cross-checked with annual bark beetle infestation data from 2017 to 2021, and only those without spatial overlap with infested areas were retained as reference data. For Sentinel-2 analysis, the selected healthy plots were rasterized to a 20 × 20 meter resolution to match the sensor's spatial resolution and subsequently converted to point data for extracting spectral reflectance values of healthy spruce canopies. For DESIS analysis, the original 30 × 30 meter plot sizes were used directly, as they align with the spatial resolution of DESIS imagery.

2.3 Extraction of Reflectance Values

Reflectance values across all infestation phases were extracted to assess spectral differences between healthy and infested canopies and to compare these variations between DESIS and Sentinel-2, addressing the first research objective. The DESIS data has a pixel size of 30x30m, and Sentinel-2 data has pixel sizes of 10m, 20m, and 60m. For the purpose of this study, all the 10 bands in Sentinel-2 were resampled to a pixel size of 20x20m. To ensure compatibility with the vectorised polygons representing bark beetle infestations, the polygons were rasterised to pixel sizes of 30m and 20m using the Polygon to Raster tool in Arcgis Pro v3.1. Polygons smaller or larger than 30m were excluded from further analysis for the DESIS data, and polygons smaller or larger than 20m were excluded from further analysis with Sentinel-2. The rasterized data was then converted into points using the Raster to Points tool in ArcGIS Pro v3.1. These points, representing the centers of the infested pixels, formed the basis for further analysis.

To extract the reflectance values for all infestation phases, the Extract Multi Values to Points tool in Arcgis Pro v3.1 was used. This tool extracts reflectance values for every pixel in the image across all spectral bands. The input point features consisted of point data representing the locations of bark beetle infestations, while the DESIS and Sentinel-2 data served as the input rasters. The process was repeated for images representing the different infestation phases: April, June, and

August. The extracted reflectance values were initially stored in dBase format and later converted to Excel format using the Table to Excel tool in Arcgis Pro v3.1
After visualising the data in Excel for DESIS, it was observed that the reflectance values associated with the wavelength range of 402 to 411.2 nm for all infestation phases had issues, such as negative values and very low values. To prevent outliers in the analysis, these wavelengths were excluded from further analysis; a total of 5 bands were removed, and 230 bands were used for further analysis. The resulting dataset was then exported into MATLAB vR2024b, where the spectral profiles for all infestation phases for both datasets were visualised and analysed. These same procedures were repeated for the healthy stands to ensure comparability.

2.4 Calculation of Red-Edge Position

In this research, the REP was calculated using polynomial fitting techniques (Pu et al., 2003), in polynomial fitting, the red-edge reflectance curves lie between the wavelength corresponding to the minimum reflectance in the red region and the maximum in the NIR region, often referred to as the 'shoulder' reflectance. The purpose of calculating REP was to see how it varies across different infestation phases. The polynomial fitting method was chosen to calculate the REP in DESIS image spectroscopy data and Sentinel-2 imagery because it accurately models the nonlinear relationship between spectral bands and reflectance values. This technique is ideal for capturing the red edge shift, which is crucial for analyzing vegetation health and characteristics (Pu et al., 2003). Polynomial fitting has been widely used in remote sensing, particularly for identifying spectral features like the red edge, and has been shown to provide reliable results in similar applications (Pu et al., 2003). This technique was originally proposed by Guyot and Baret (1988) to detect chlorophyll-related shifts in vegetation spectra and has since been applied to forest health monitoring by Pu et al. (2003). It is not only computationally efficient but also easy to interpret, making it suitable for processing large datasets such as those from Sentinel-2 and hyperspectral sensors. Given its effectiveness in previous studies, it was the most preferred method to be used in this study, given the kind of datasets that were used in this study. In MATLAB vR2024b, the REP was calculated using polynomial fitting techniques. A fifth-degree polynomial was fitted to the reflectance values within the red-edge spectral range (680–750 nm) for each pixel. This order of polynomial provides flexibility to capture the curvature in the red-edge region without overfitting (Pu et al., 2003). To find the REP, the maximum of the first derivative of the polynomial function was identified, as demonstrated in the equation below.

$R(\lambda) = a_0 + \sum_{i=1}^{5} a_i \lambda^i$ ………………………………………………………… Equation 1

Where $R(\lambda)$ represents the reflectance at specific wavelengths, a_0-a_5 are the coefficients of the fifth-order polynomial and λ represent the wavelength of the sensor.

2.5 Selecting Significant Spectral Bands

Identifying the green phase of infestation is critical for monitoring the spread of infestation to other Norway spruce stands (Kautz et al., 2023). Detecting this phase enables timely management and removal of infested species, which helps prevent the spread of infestation. The purpose of performing the ANOVA test in this study is to assess which spectral regions or bands in DESIS and Sentinel-2 data can distinguish between canopies under bark beetle stress (green attack) and healthy canopies, as well as to evaluate the potential of using these bands to map bark beetle green infestations. To achieve this, a one-way ANOVA test was conducted to identify the spectral bands that exhibit significant differences between healthy and infested Norway spruce stands. Before conducting the ANOVA test, the Shapiro-Wilk test was applied to ensure that the data followed a normal distribution. The test resulted in a p-value greater than 0.05, confirming that the data were normally distributed, satisfying the assumption of normality required for the ANOVA test.

ANOVA is widely used in hyperspectral and multispectral data analysis to evaluate spectral separability and identify the most informative bands for classification and feature selection (Mutanga & Skidmore, 2004). In this study, the one-way ANOVA test was used to evaluate whether the means of healthy and infested canopies were statistically different by comparing between-group and within-group variability. According to Kim (2017), the one-way ANOVA test is given by two major components, intergroup and intragroup.

Intergroup variation refers to the differences between the means of different groups. It shows how much the groups differ from each other overall, which is given by;

$$\sum_{i=1}^{k} n_i \left(\overline{Y}_i - \overline{Y}\right)^2 / (K - 1) \quad \ldots\ldots \quad \text{Equation 2}$$

Intragroup variation refers to the differences within each group, showing how much individual values vary around their group mean, which is given by

$$\sum_{ij=1}^{n} \left(\overline{Y}_{ij} - \overline{Y}_i\right)^2 / (N - K) \quad \ldots\ldots \quad \text{Equation 3}$$

To perform one-way ANOVA, test the intergroup is therefore divided by intragroup.

$$F = \frac{\sum_{i=1}^{k} n_i \left(\overline{Y}_i - \overline{Y}\right)^2 / (K-1)}{\sum_{ij=1}^{n} \left(\overline{Y}_{ij} - \overline{Y}_i\right)^2 / (N-K)} \quad \ldots\ldots \quad \text{Equation 4}$$

Where: $\overline{Y}_i$is the mean of the group i; n_i is the number of observations of group i; $\overline{Y}$ is the overall mean; K is the number of groups; $\overline{Y}_{ij}$ is the jth observational value of group i; and N is the number of all observational values. The F statistic refers to the result of the test. This equation was implemented in MATLAB vR2024b, and test was performed with a confidence level set at $P > 0.05$ and was applied band to band across all 230 spectral bands in the DESIS data and 10 bands in the Sentinel-2 data. Bands with p-values greater than or equal to 0.05 were considered insignificant for distinguishing between healthy and infested canopies. The test identified spectral bands with p-values less than 0.05 as significant for distinguishing between healthy and infested trees. These significant bands were further utilized for mapping the green phase of infestation.

2.6 Mapping early-stage bark beetle infestation (Green Attack)

The second research objective of this study focuses on mapping early-stage bark beetle infestations using bands identified as significant by the ANOVA test, along with a combination of vegetation indices. The workflow for this objective includes selecting appropriate vegetation indices, training RF model, and finally assessing the model's performance.

2.6.1 Vegetation Indices (VIs)

The VIs used in these studies are NDRE(Normalized Difference Red Edge Index), (Gitelson, et al 1994), GNDVI (Green Normalized Difference Vegetation Index), (Gitelson et al 1996) , NDWI (Normalized Difference Water Index), (Goa et al., 1996) , MSAVI (Modified Soil Adjusted Vegetation Index), (Qi et al., 1994) , and MNDWI (Modified Normalized Difference Water Index), (Xu, 2006); these indices were selected because they are sensitive to detecting stress induced by different stressors, such as insects, drought, and heat waves. NDRE is especially effective at detecting changes in chlorophyll content, particularly in the red-edge region of the spectrum, which is critical in identifying the early stages of infestation when trees begin to show subtle signs of chlorophyll degradation (Gitelson et al., 1994). On the other hand, GNDVI is sensitive to the green reflectance in vegetation, allowing it to capture the interaction between chlorophyll and leaf structure. As bark beetles affect leaf health, causing discolouration and damage, GNDVI is a valuable index for assessing the health of vegetation and chlorophyll concentration during early infestation (Gitelson et al., 1996). NDWI is another key index that helps detect changes in water content in plant tissues. As bark beetles invade trees, they often reduce the plant's ability to retain water, and NDWI is ideal for monitoring this physiological stress (Gao, 1996). MSAVI is one of the most widely used indices for monitoring vegetation health, particularly in areas where soil background effects can influence spectral signals. MSAVI improves upon traditional vegetation indices by incorporating a soil brightness correction factor, allowing for more accurate assessment of vegetative health in areas with sparse to moderate vegetation cover. It measures the difference between NIR and red reflectance, like NDVI, but is specifically designed to minimize soil influence. In the context of bark beetle infestations, MSAVI is especially useful for detecting early signs of stress in forest vegetation before visible symptoms become prominent. This makes it a valuable index for identifying subtle but widespread patterns of infestation in forested landscapes, including those in heterogeneous or disturbed environments (Qi et al., 1994). Finally, MNDWI focuses on detecting moisture levels in vegetation. As bark beetles attack, they cause trees to lose moisture, and MNDWI is particularly sensitive in identifying the loss of moisture content in the plants. This index is handy for early detection of beetle damage, as it is more responsive to changes in vegetation moisture than traditional indices (Xu, 2006). In a nutshell, these indices provide complementary information on different aspects of tree health, such as chlorophyll content, moisture levels, and overall vegetation stress, making them ideal for detecting early-stage bark beetle infestations. Using both Sentinel-2 and DESIS, these indices will be calculated and used as input features in the RF model. These indices are further summarized in table below with their respective equations.

Table 4: Lists of Vegetation Indices used in the RF Model

Indices	Equations	Source	
NDRE1	$\frac{R_{NIR} - R_{RED\ EDGE}}{R_{NIR} + R_{RED\ EDGE}}$	Gitelson, et al (1994)	Equation 5
GNDVI	$\frac{R_{NIR} - R_{GREEN}}{R_{NIR} + R_{GREEN}}$	Gitelson et al (1996)	Equation 6
NDWI	$\frac{R_{GREEN} - R_{NIR}}{R_{GREEN} + R_{NIR}}$	Goa et al., (1996)	Equation 7
MSAVI	$\frac{2NIR + 1 - \sqrt{(2NIR + 1)^2 - 8(NIR - RED)}}{2}$	Qi et al., (1994)	Equation 8

MNDWI	$\frac{R_{GREEN} - R_{SWIR}}{R_{GREEN} + R_{SWIR}}$	Xu, (2006)	Equation 9

2.6.2 Random Forest Model

Early-stage infestation mapping was conducted using June imagery from Sentinel-2 and DESIS to capture the spectral signatures characteristic of green attack. RF models were developed: The first model (Model A) combined significant bands from ANOVA test and vegetation indices (VIs) for each dataset (one model for DESIS and one for Sentinel-2). The second model (Model B) used only the bands identified as significant by an ANOVA test (again, one model for DESIS and one for Sentinel-2). Each dataset thus had two main models: Model A, which combined significant bands from ANOVA test and VIs separately for each dataset, and Model B, which included only the significant bands identified by the ANOVA test for each dataset.

The aim of using two RF models was to assess the impact of including vegetation indices in the classification process for both DESIS and Sentinel-2 data and to evaluate the role of VIs in distinguishing between healthy and infested spruce canopies. The RF algorithm was chosen for the classification process due to its efficiency in handling high-dimensional datasets and its ability to identify complex relationships between target classes and input features (Krstajic et al., 2014).

Using Google Earth Engine, classification began by importing June imagery, healthy spruce stand, and bark beetle infestation datasets as assets. The healthy spruce stand and bark beetle infestation datasets were used to train the RF classifier. Seventy percent (70%) of the labeled data were used for training the model, and the remaining thirty percent (30%) was reserved for testing its performance. Since the Bavarian Forest National Park (BFNP) is a multi-species environment, precautions were taken to prevent over-prediction of infestation in the RF. Non-coniferous forest species were masked out to ensure the model applied only to coniferous species, which are susceptible to bark beetles. After training, the model was applied across the entire June dataset, considering only coniferous forests. The two datasets, DESIS and Sentinel-2, produced four binary infestation maps, two for each of the two models: one using vegetation indices and reflectance from significant bands for each dataset, and another using only the reflectance from significant bands identified for each dataset.

2.6.3 Assessment of the model performance.

The accuracy of the classification was assessed using confusion matrices. The reserved validation dataset was classified using the RF model, and the predicted labels were compared to the actual reference labels. Confusion matrices were generated to evaluate the model's performance on the two datasets, providing key metrics such as overall accuracy and kappa coefficient. These metrics were critical in identifying misclassification patterns and assessing the robustness of the model across different classes. The integration of Random Forest classification, feature importance analysis, and confusion matrix evaluation ensured a reliable and comprehensive approach to mapping green-phase infestation. According to Story et al., (1986), producer and user accuracy can be calculated using the following formulas

User accuracy = $\frac{TP}{TP+FP}$ ……………………………………………………... Equation 10

Producer accuracy =$\frac{TP}{TP+FN}$ …………………………………………………….. Equation 11

Where:

TP is true positive (correctly classified pixels for a given class), FP is false positive (pixels incorrectly classified as a given class) and FN is false negatives (pixels that belong to a class but were misclassified as another class. Although the RF produces confusion matrices for the two datasets, however these matrices were not presented in the results section because there were misleading for example, the models that over -predicted bark beetles green attack were having higher level of overall accuracy, for this reason ,verifications were done manually using the infestation reference data and the above equations from (Story, et al., 1986). This was achieved by comparing the model-identified green attack pixels to the reference data, enabling the evaluation of how many detected pixels accurately corresponded to actual green attack areas.

3 RESULTS

This chapter provides an overview of the results generated from the application of the methodology discussed in the previous chapter. The section is structured into five subsections, each corresponding to a different component of the research objectives.

- The first subsection presents the findings from the extraction of reflectance data for healthy and infested canopies across all stages of infestation.
- The second subsection presents the findings from the second part of objective one, which involves selecting significant spectral bands to map the bark beetles green attack.
- The third subsection presents the findings from the final section of objective one , calculation of the red edge position for all stages of infestation.
- The fourth subsection presents the findings from the Random Forest classification of bark beetle green attacks, along with an assessment of the model's performance, which is objective two.

3.1 Variability of Canopy Reflectance Before and During Bark Beetle Infestation

The spectral reflectance before infestation in April was extracted for both DESIS and Sentinel-2. Figures 3 and 4 display the mean reflectance of selected canopies before infestation and healthy canopies in April for DESIS and Sentinel-2, respectively. For DESIS, the mean reflectance of the two canopies shows similarities across the entire spectrum (400 nm to 1000 nm), as shown in Figure 3. Both canopies exhibit low reflectance in the visible region (400 nm–700 nm) and higher reflectance in the NIR region (700 nm–1000 nm).

In contrast, a different pattern was observed in Sentinel-2, as shown in Figure 4. There is a significant difference between the curves of the two canopies across the entire spectrum (440 nm–2200 nm). The pre-infestation canopies show higher reflectance in both the visible region of the spectrum (450 nm–650 nm) and NIR (800 nm–2200 nm). The reflectance of healthy canopies was generally lower across the entire spectrum, except in the red-edge region (650 nm–740 nm), where higher reflectance was observed.

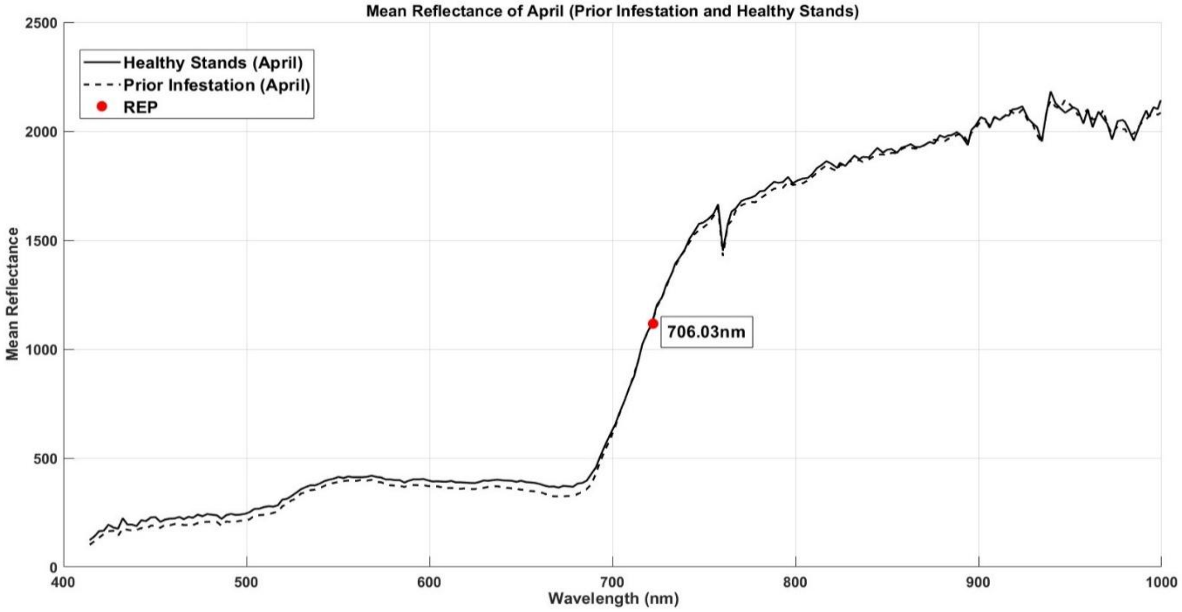

Figure 3: Mean DESIS spectral reflectance of pre-infested (canopy patches that were later infested in June), and healthy spruce stands in BFNP in April 2021, with the location REP indicated

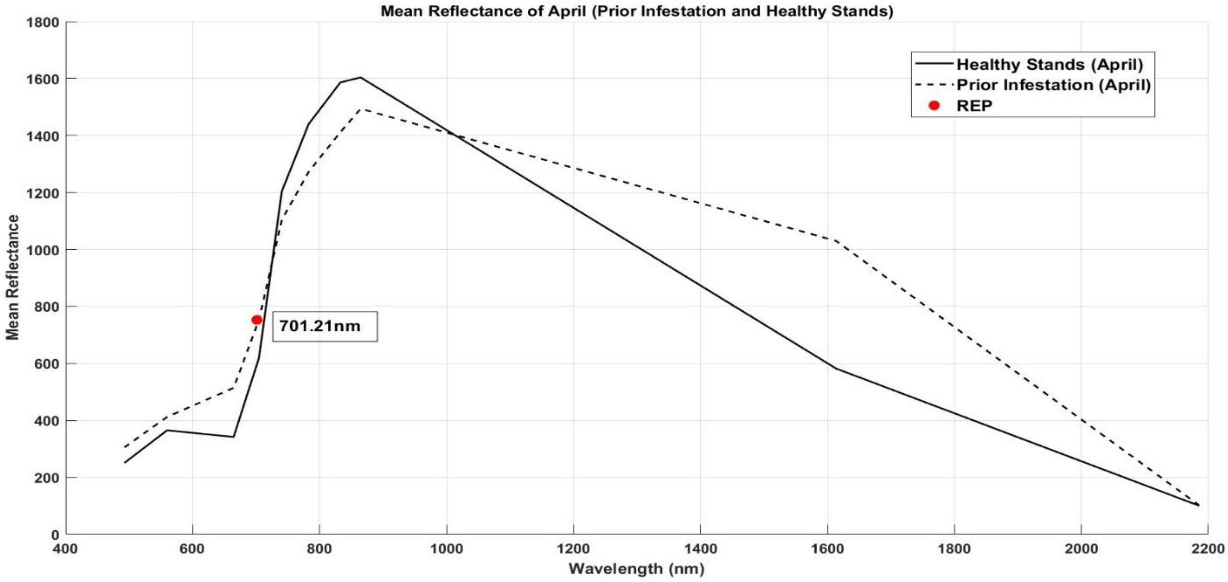

Figure 4: Mean Sentinel-2 spectral reflectance of pre-infested (canopy patches that were later infested in June), and healthy spruce stands in BFNP in April 2021, with the location REP indicated.

Figures 5 and 6 display the mean reflectance of canopies under bark beetle green attack and healthy stands in June for DESIS and Sentinel-2, respectively. For DESIS, as shown in Figure 5, the reflectance of canopies under green attack was elevated within the red-edge spectral range (590 nm–700 nm) of the spectrum and lower in the NIR (750 nm–1000 nm). Both canopies exhibited a similar trend in the visible region (450 nm–600 nm). The reflectance of healthy stand canopies was generally higher in the NIR region and lower in the red-edge region.

A completely different pattern was observed in Sentinel-2, as displayed in Figure 6. The canopies under bark beetle green attack showed higher reflectance in the visible region (450 nm–650 nm), NIR, and SWIR, except in the red-edge region, where the reflectance of both canopies was similar. The reflectance of healthy stands was lower in the visible region, NIR, and SWIR, which is the opposite of the reflectance of canopies under green attack.

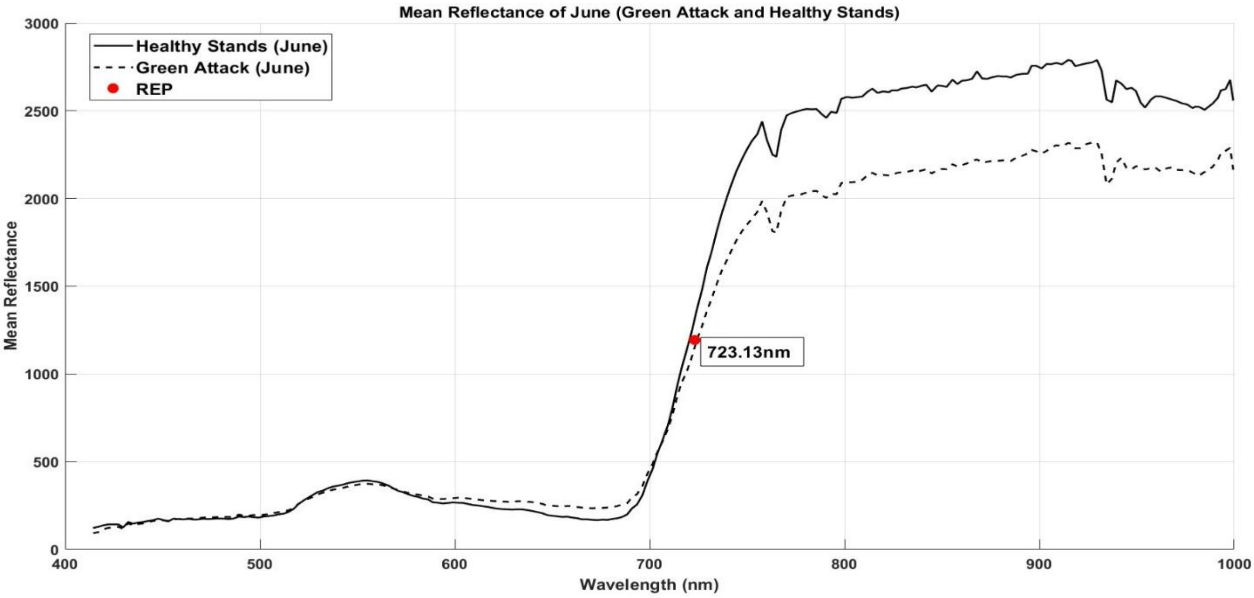

Figure 5: DESIS mean reflectance of healthy and infested canopies during the green attack in June 2021, with the location REP indicated

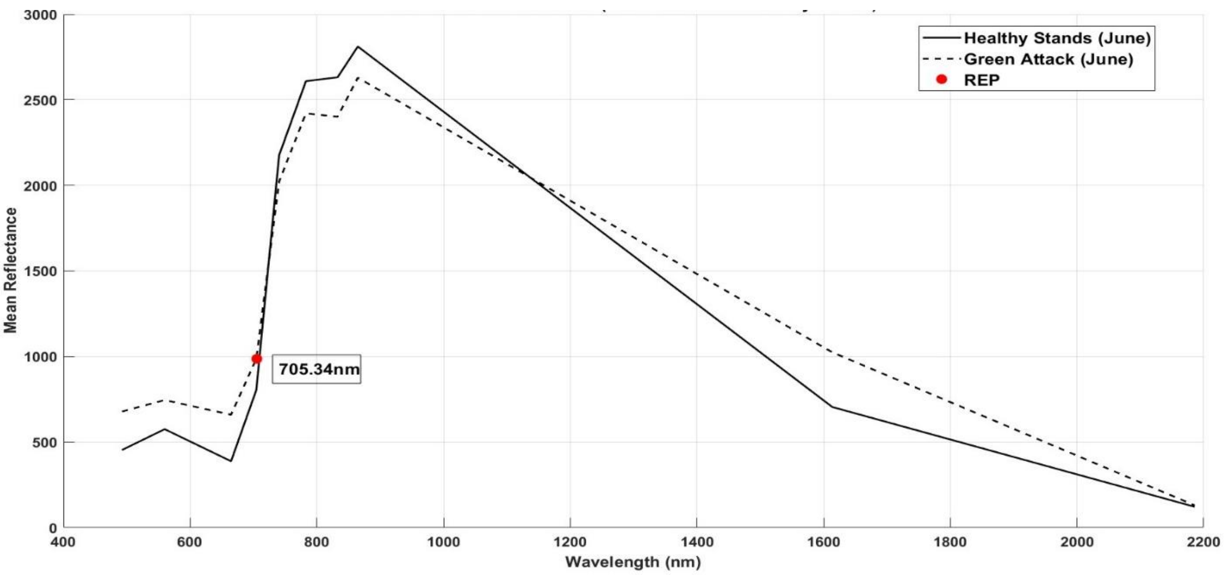

Figure 6: Sentinel-2 mean reflectance of healthy and infested canopies during the green attack in June 2021, with the location REP indicated

Figures 7 and 8 show the mean reflectance of healthy stands and canopies under red attack from bark beetle infestation in August for DESIS and Sentinel-2, respectively. For DESIS, the mean reflectance of canopies under bark beetle red attack was generally higher in the visible and red-edge regions of the spectrum (400 nm–600 nm) and (640 nm–750 nm), respectively, and lower in the

NIR (750 nm–1000 nm), as shown in Figure 7. Healthy stands exhibited the opposite pattern, with lower reflectance in the visible and red-edge regions and higher reflectance in the NIR region.
In Sentinel-2, the canopies under red attack generally showed higher reflectance across the entire spectrum, from the visible region through to the red-edge region, NIR, and SWIR. The reflectance of healthy stands was the direct opposite of the canopies under red attack, with lower reflectance across the entire spectrum, from the visible region to SWIR, as demonstrated in the figure.

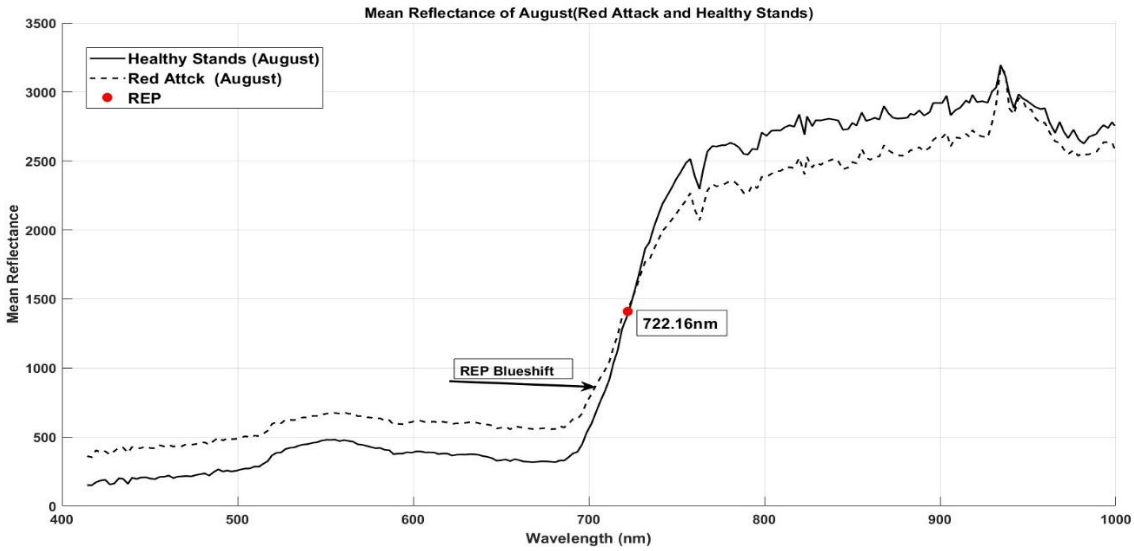

Figure 7: DESIS mean reflectance of healthy and infested canopies during the red attack in August 2021, with the location REP indicated

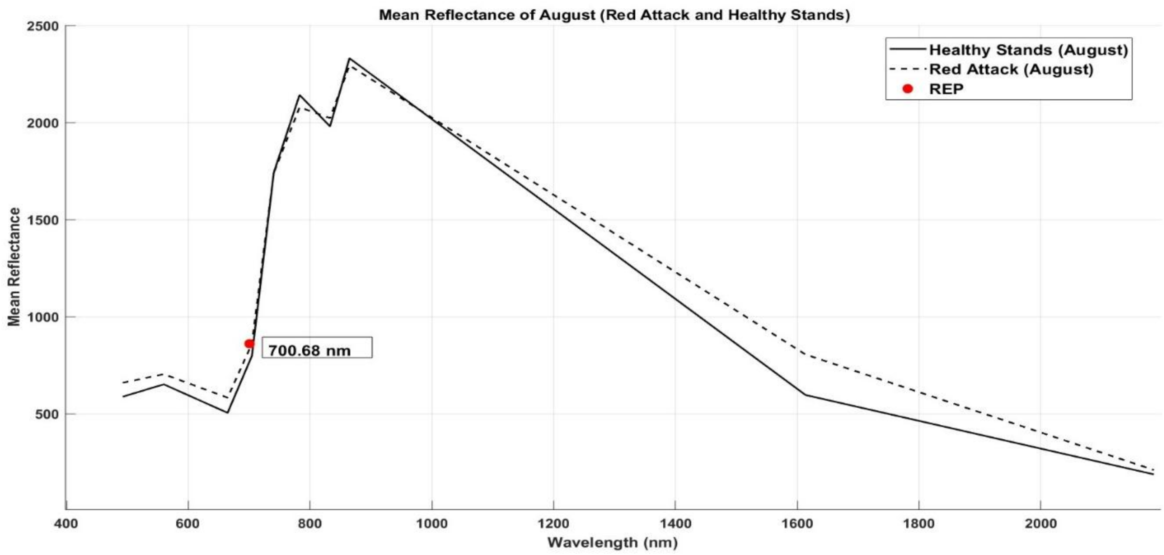

Figure 8: Sentinel-2 mean reflectance of healthy and infested canopies during the red attack in August 2021, with the location REP indicated

3.2 Selecting Significant Spectral bands.

The objective of this section of the research was to identify the key spectral bands most significant for mapping the green attack phase of bark beetle infestation. The methodology used to achieve this is described in detail in Section 4.5. The results for DESIS are presented in Figure 9, the diagram emphasizes the mean reflectance curves of the two canopies, green attack and healthy stands for the month of June. The areas shaded in pink denote spectral bands where the differences between the reflectance of the two canopies are statistically significant ($p < 0.05$). These significant bands extend across both the visible, red-edge and NIR regions, with notable clusters observed in the red-edge region (700–750 nm) and portions of the NIR region (750–1000 nm), revealing the fact that bands form red edge regions and NIR are generally sensitive to detecting early-stage bark beetles activities in vegetation.

For Sentinel-2 the results are presented in Figure 10, from the diagram the pink shaded bars represent the spectral bands that are significant ($p<0.05$) to differentiating the two canopies. From the figure the significant bands span across the visible region, red edge region NIR and SWIR, with majority of the band concentrated at the red edge region.

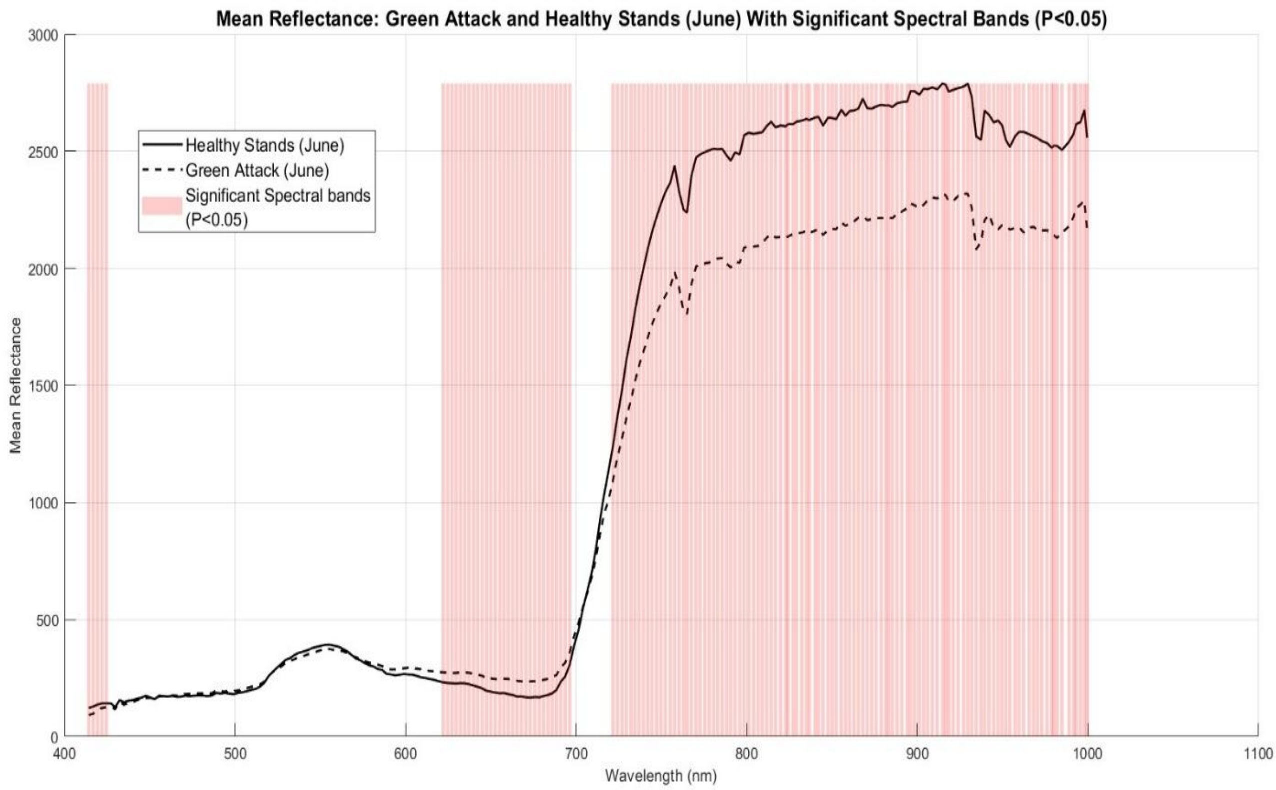

Figure 9: DESIS significant spectral bands/regions for mapping bark beetles infestation (green attack) in June

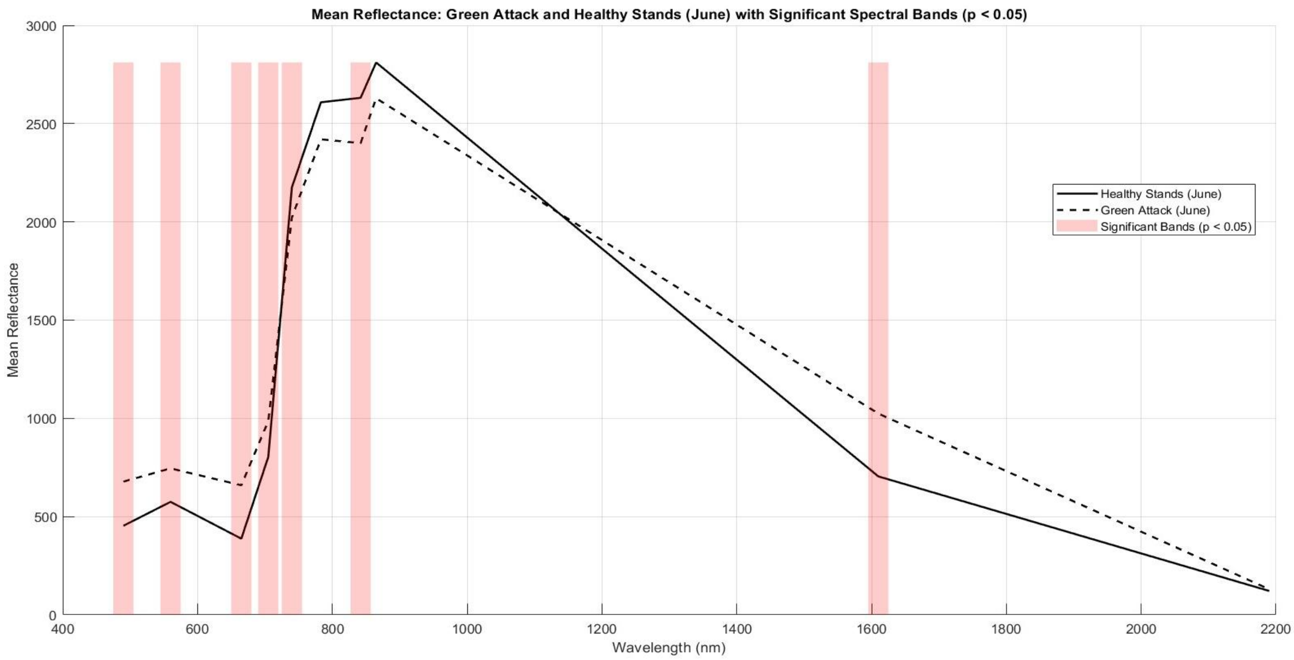

Figure 10: Sentinel-2 Significant spectral bands/regions for mapping bark beetles infestation (green attack) in June

3.3 Red Edge Positions (REP)

As part of the first research objective in this study, the position of the red edge was calculated for all stages of bark beetle infestation using both DESIS and Sentinel-2 data. The purpose of calculating the REPs was to assess how they vary across different phases of infestation. For DESIS, the REP was identified at 706.03 nm, 723.13 nm, and 722.16 nm for the prior infestation phase in April, green attack in June, and red attack in August, respectively. These positions are indicated by red dots on the spectral curves in Figures 3, 5, and 7. For Sentinel-2, the red edge positions were observed at 701.21 nm, 705.34 nm, and 700.60 nm for the same respective periods. These positions are marked by red dots on the spectral curves in Figures 4, 6, and 8. REP is a key indicator in identifying vegetation under stress caused by bark beetle activity.

When vegetation is photosynthetically active and healthy, the REP tends to shift toward longer wavelengths. Conversely, when vegetation is under stress, the REP shifts toward shorter wavelengths. In April, the REP for DESIS was measured at 706.03 nm, indicating that the vegetation are photosynthetically actives, which serve as a main indicator for healthy vegetations.

In June, during the green attack phase, the REP shifted to 723.13 nm for DESIS and 705.34 nm for Sentinel-2. However, by August, during the red attack phase, the REP slightly shifted back to shorter wavelengths 722.16 nm for DESIS and 700.60 nm for Sentinel-2, This trend reinforces that as bark beetle infestation intensifies, photosynthesis decreases, and the REP moves toward shorter wavelengths.

3.4 Mapping Early-Stage Bark Beetles Infestation (Green Attack)

The second objective of this research was to map bark beetle green-attack infestations using two strategies: one combining reflectance from significant bands with vegetation indices, and the other relying solely on those spectral bands deemed significant by ANOVA testing. These models were applied to both DESIS and Sentinel-2 data. Based on these input features, two RF models were developed to generate infestation maps representing bark beetle green attacks for both datasets. The generated maps were compared against ground truth data (aerial photography) to evaluate pixel-level agreement and disagreement with actual infestation locations. Figures 11 and 12 show the correctly classified pixels that matched the ground truth, as well as those misclassified by the RF models for Model A and Model B, respectively.

Model A's assessment results are presented in Table 5. For DESIS, 733 pixels (47%) correctly matched the ground truth (reference infestation data), compared to 1,476 pixels (41%) for Sentinel-2. Conversely, the number of mismatched or incorrectly classified pixels was lower for DESIS, with 835 pixels (53%), compared to 2,096 pixels (59%) for Sentinel-2.

Table 6 presents the assessment results for Model B. For DESIS, 728 pixels (46%) correctly matched the ground truth, whereas Sentinel-2 achieved only 325 pixels (9%). Similarly, DESIS had fewer misclassified pixels, 804 (54%), compared to Sentinel-2, which had 3,220 pixels (91%).

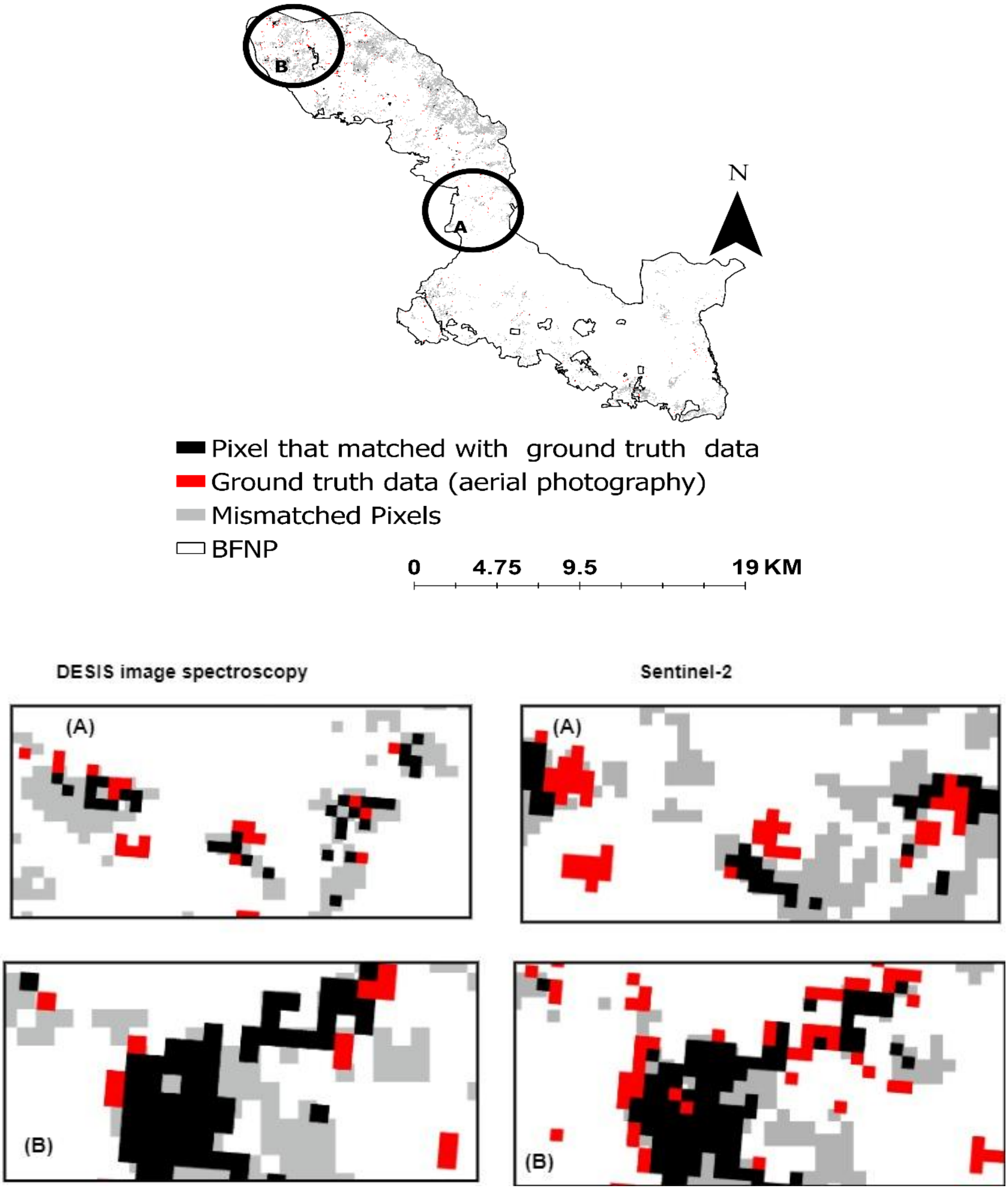

Figure 11: Map showing the spruce canopies under bark beetles green-attack in Bavarian Forest National Park in June 2021, Based on Random Forest Classification from DESIS Image Spectroscopy and Sentinel-2, for Model A (The combination of significant bands from ANOVA test and Vegetation indices)

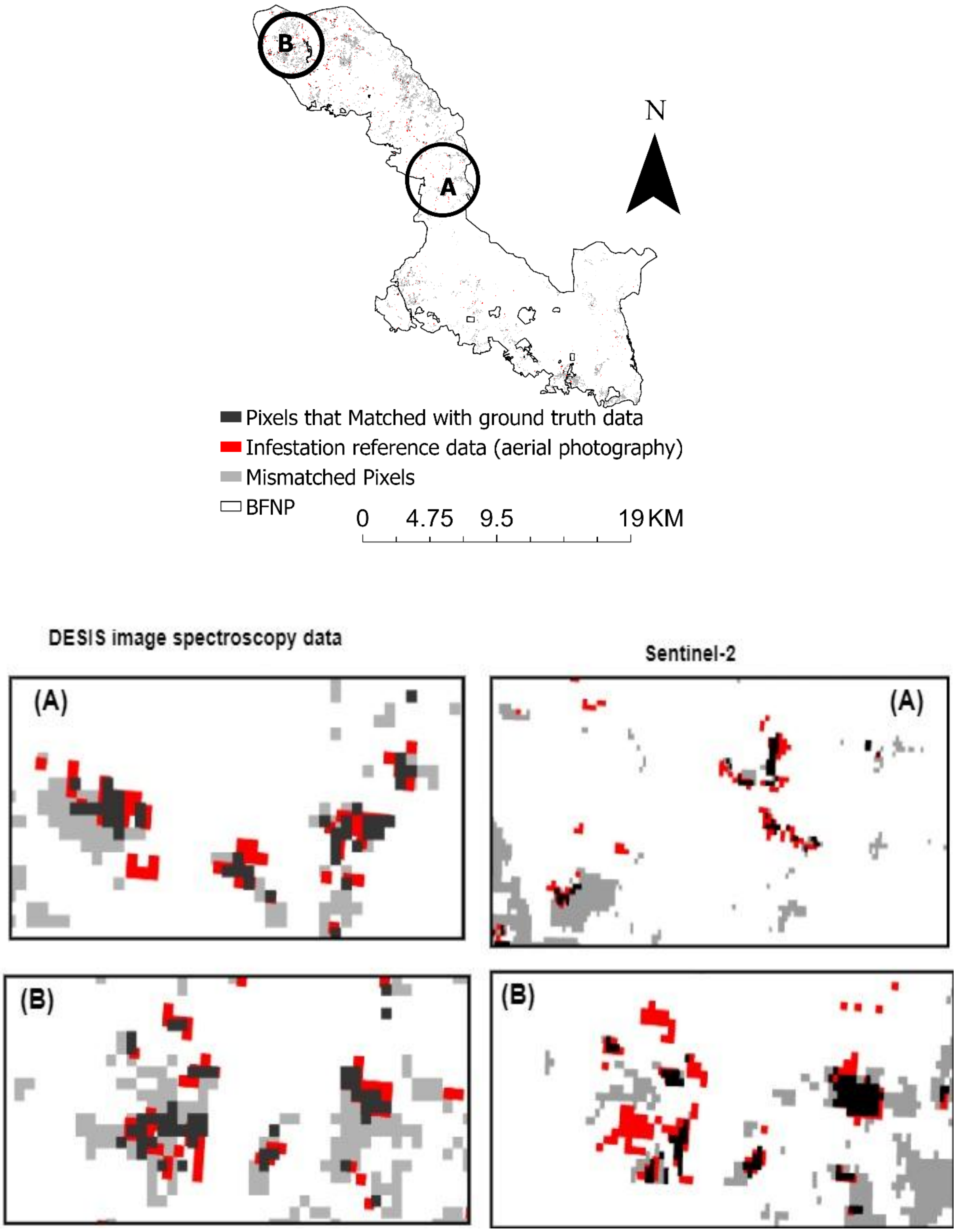

Figure 12: Map showing the spruce canopies under bark beetles green-attack in Bavarian Forest National Park in June 2021, Based on Random Forest Classification from DESIS Image Spectroscopy and Sentinel-2, for Model B (Only significant bands from the ANOVA test)

Table 5: Assessment of the generated maps from DESIS image spectroscopy and Sentinel-2 from RF model using the reference data obtained from Aerial Photography for Model A (Combination of significant bands from ANOVA test and vegetation indices)

Identified Pixels as green attack	Reference pixels (Aerial photography)	Pixels Correctly matched	Mismatched Pixels	Differences
DESIS (22,634 pixels)	1, 568 (30m)	733 (47%)	835	53%
Sentinel2 (39,027)	3,572 (20m)	1,476(41%)	2,096	59%

Table 6: Assessment of the generated maps from DESIS image spectroscopy and Sentinel-2 from RF model using the reference data obtained from Aerial Photography for Model B (only the bands identified by the ANOVA test as significant)

Identified Pixels as green attack	Reference pixels (Aerial photography)	Pixels Correctly matched	Mismatched Pixels	Differences
DESIS (15,274 pixels)	1, 568 (30m)	728 (46%)	840	54%
Sentinel2 (15,146)	3,572 (20m)	325 (9%)	3,220	91%

4. DISCUSSION

This study focused on detecting and mapping bark beetle infestations during green attack in the Bavarian Forest National Park, Germany using Sentinel-2 and DESIS image spectroscopy data. It is the first study to utilize DESIS image spectroscopy data to detect bark beetle infestations at the canopy level during green attack. The study showed that DESIS and Sentinel-2 spectral bands , particularly the bands from the red-edge and NIR regions can to some extent map the bark beetle green attack. The RF classification revealed that DESIS data outperformed Sentinel-2 in detecting bark beetle infestation.

4.1 Variations of Canopy Spectral Reflectance between Healthy and Infested Norway Spruce Stands

Both DESIS and Sentinel-2 data provided significant insights into the developmental stages of bark beetle infestation and its impact on the spectral characteristics of Norway spruce stands. Subtle physiological and biochemical changes in Norway spruce canopies caused by bark beetle infestation were clearly detectable in DESIS hyperspectral data, especially in the red-edge and NIR regions (Figure 9). In contrast, these changes were only partially observable in the red-edge region of the Sentinel-2 data (Figure 10). This subsection discusses the variations in spectral reflectance between healthy and infested Norway spruce canopies across the bark beetles stages examined in this study: prior to infestation, during the green attack, and during the red attack. It also compares the spectral reflectance patterns captured by DESIS and Sentinel-2 across the infestation stages.

4.1.1 Prior Infestation

In April, the mean reflectance of healthy canopies and those prior to infestation i.e. canopies that were later infested in June, exhibited lower reflectance in the visible region and higher reflectance in the NIR region. The lower reflectance in the visible region can be attributed to chlorophyll absorption, a key indicator of healthy vegetation (Yoder & Waring, 1994). In contrast, healthy vegetation typically shows strong reflectance in the NIR region because of an increase in scattering of electromagnetic radiation in the NIR region, as noted by Abdullah et al. (2018). This likely explains the elevated NIR reflectance observed in April, before the bark beetle swarming began in the spruce stands.

There were no notable differences detected between the two canopies in the DESIS data (Figure 3). However, Sentinel-2 data revealed noticeable differences between them (Figure 4). These discrepancies in reflectance can be attributed to the different sensor characteristics, including spectral, spatial, and temporal resolution. Sentinel-2 has a lower spectral resolution, offering only 13 bands compared to DESIS's 235 bands. This likely explains why Sentinel-2 was less capable of detecting subtle differences between the two canopy types. This limitation has been highlighted in literature. For example, Morin et al. (2017) emphasized that sensor resolution and band configuration significantly influence the sensitivity of spectral curves to vegetation health, particularly under stress conditions such as pest infestations. Additionally, temporal differences such as weather conditions or changes in canopy characteristics like leaf area index may also contribute to the observed differences, since the two datasets were acquired on different dates.

This issue was also noted by Osińska-Skotak et al. (2019), who reported that the timing of data acquisition affects the ability to distinguish plant species during vegetation succession.

4.1.2 Green Attack

During the green attack stage, healthy canopies continue to exhibit reflectance patterns like those observed prior to infestation, characterized by lower reflectance in the visible region (400nm to 600nm) and higher reflectance in the near-infrared (NIR) region (700nm to 1000nm). In contrast, canopies affected by bark beetle green attack display higher reflectance in the visible region and reduced reflectance in the NIR region (Figures 5 and 6). Bark beetles primarily target the phloem tissue of spruce forest, which is responsible for transporting nutrients from the roots to the leaves (Felicijan et al., 2015). As the infestation progresses, the phloem tissue becomes severely damaged, disrupting nutrient flow. This deprivation leads to chlorophyll degradation and structural damage in the canopy, resulting in increased reflectance in the visible region and decreased reflectance in the NIR due to the breakdown of internal leaf structure (Lausch et al., 2016; Hais et al., 2016).
DESIS data successfully distinguished between canopies under bark beetles green-attacked and healthy canopies in the red-edge, and near-infrared regions (Figure 5). Sentinel-2 was also able to detect bark beetle green attacks to some extent, particularly in the red-edge region (Figure 6). However, no notable differences were observed between the two canopies in the visible region, specifically in the blue wavelengths (400–500 nm), for either dataset. This is likely because reflectance in these wavelength ranges is insufficient to differentiate between healthy and stressed canopies under bark beetle green attack, a challenge also noted by Abdullah et al. (2018). For Sentinel-2, bands in the SWIR region could not distinguish between green-attacked and healthy canopies. This limitation is probably because bark beetle green attacks primarily affect foliar reflectance and biochemical properties, making it difficult to separate healthy from affected canopies in the SWIR region, as also highlighted by Abdullah et al. (2018).

4.1.2 Red Attack.

During the red stage of infestation, the affected spruce trees begin to exhibit visible symptoms, such as reddish canopies. At this stage, the tree's internal systems, particularly the phloem tissue and chlorophyll, are completely destroyed, leading to a cessation of chlorophyll production (Marx, 2010). As a result, there is increased reflectance in the visible region and decreased reflectance in the NIR region, as the damaged canopies lose their structural integrity and scattering properties (Luo et al., 2023). This trend is evident in the DESIS data, which shows higher reflectance in the visible and red-edge regions and lower reflectance in the NIR region (Figure 7). Sentinel-2 data also reflects a similar pattern, with the exception of the SWIR region, where canopies under red attack exhibit higher reflectance than healthy canopies (Figure 8).
Throughout these stages, DESIS consistently noticed these changes with greater precision, particularly at red-edge and NIR regions. Its fine spectral resolution gave it a clear advantage. While Sentinel-2 captured the general trends well, it struggled to detect the more subtle physiological shifts, especially in the visible and SWIR ranges. In the end, DESIS proved to be the more dependable tool for monitoring and identifying bark beetle infestations, especially useful for early detection and in-depth canopy analysis.

In conclusion DESIS data revealed better patterns compared to Sentinel-2, in how Norway spruce canopies respond to bark beetle attack at various stages in the Bavarian Forest National Park. Before the beetles struck, healthy and soon-to-be-affected trees looked much the same, showing the typical pattern for healthy vegetation, low reflectance in the visible spectrum due to chlorophyl absorption and strong reflectance in the NIR. As the infestation moved into the green-attack phase, infested trees began to reflect more light in the visible range and less in the NIR, a shift linked to damage in the phloem tissue and the breakdown of chlorophyll. These changes became even more pronounced during the red-attack stage, when internal damage was severe leading to significantly higher reflectance in the visible and red-edge reflectance and much lower reflectance in the NIR.

4.2 Variations of Red Edge Position (REP) across Different Phases of Bark Beetles Infestation

This subsection discusses results on how the Red Edge Position (REP) varies across different stages of bark beetle infestation and compares how this position differs between DESIS image spectroscopy and Sentinel-2 data.

4.2.1 REP and Prior Infestation.

The REP prior to infestation was measured at 706.03 nm and 701.21 nm for DESIS and Sentinel-2 respectively, indicating healthy and active vegetation. According to Hellwig et al. (2021), the REP for healthy vegetation typically lies between 700 and 750 nm, although this value may vary depending on the plant species and sensor properties such as the spectral resolutions. A shift of REP toward longer wavelengths suggests ongoing photosynthetic activity. In the BFNP, bark beetles typically begin to swarm in spruce stands when the temperatures reach 16.5°C in the daytime, according to Marx, (2010). However, based on weather data from Waldhauser, a local weather station in BFNP , average temperatures in the region in 2021 during April was 4.1°C and highest was less than 16.5°C during the day for sustained periods. This explains why the vegetation in April appears to be in its natural state, unaffected by bark beetle activity.

4.2.2 REP and Bark Beetles Green Attack.

During the green attack stage, we expected the Red Edge Position (REP) to shift toward shorter wavelengths compared to its position before infestation, as this usually indicates vegetation stress and reduced photosynthetic activity caused by chlorophyll degradation (Felicijan et al., 2015). However, unlike previous studies (Velichkova et al., 2019; Jung et al., 2006), which observed a REP shift toward shorter wavelengths in stressed vegetation, our findings showed the opposite: the REP shifted toward longer wavelengths723.13 nm for DESIS and 705.34 nm for Sentinel-2. This unexpected result could be because, in June, the level of chlorophyll degradation was not yet significant enough to cause a shift toward shorter wavelengths. As shown in Figure 5, the mean reflectance curves of healthy and infested canopies in DESIS data in June are quite similar in some part of the red-edge region (700–730 nm). This phenomenon has also been acknowledged in other studies. For example, Huo et al. (2022) observed that spectral differences between healthy and green-attacked spruce forests were not noticeable in the early stages when using Sentinel-2 and WorldView imagery. They explained that green attacks do not show spectral differences unless those differences already exist before the infestation. Similarly, Fernández et al. (2020) found no REP shift toward shorter wavelengths in cases of potato late blight when using a Micasense® Dual-

X camera. They also suggested this was due to insufficient chlorophyll degradation to trigger a noticeable spectral change. This study therefore conclude that the REP positions measured in DESIS and Sentinel-2 was not good indicator for detecting Norway spruce forest under bark beetles green attack in BFNP in 2021.

4.2.3 REP and Bark Beetles Red Attack.

The red attack phase represents the advanced stage of bark beetle infestation. At this stage, infested Norway spruce trees begin to exhibit symptoms such as reddish canopies, indicating the complete breakdown of chlorophyll and the cessation of photosynthetic activity. The REP during this phase is expected to shift further toward shorter wavelengths when compared to the green attack phase. In this study, this phenomenon was observed in both DESIS (Figure 7) and Sentinel-2 data (Figure 8), where REP values shifted to 722.16 nm and 700.68 nm, respectively. This shift aligns with findings by Carter and Knapp (2001), who associated such changes with reduced chlorophyll content and degradation of cell structure. These physiological changes lead to a complete halt in photosynthesis, causing the spectral signature of the affected trees to show increased reflectance in the visible region and decreased reflectance in the NIR and SWIR regions typical characteristics of dead vegetation.

To summarize how the REP varies across different bark beetle infestation phases: Before the infestation, REP values indicated healthy vegetation, reflecting normal photosynthetic activity. However, during the green attack phase, REP shifted unexpectedly toward longer wavelengths, which did not align with previous studies. This unusual shift may have occurred because chlorophyll degradation had not progressed significantly by June, so the spectral difference between healthy and infested trees was still minimal. Once the red attack phase began when the trees were visibly stressed and losing chlorophyll REP values shifted back toward shorter wavelengths, consistent with what past research has observed for stressed vegetation.

4.3 Significant Spectral Differences Between Healthy and Infested Canopies Identified by the ANOVA Test

The ANOVA test identified a number of significant bands (p-value < 0.05) related to the detection of green attack phase of bark beetle infestation. Most of these bands in the DESIS dataset were identified in the red-edge spectrum (approximately 650–750 nm) and the NIR spectrum (750–1000 nm). Sentinel-2 results showed major bands mainly in the red, red-edge, and near-infrared (NIR) spectrum (500–850 nm), and one major band in the SWIR spectrum. These results are presented in Figures 9 and 10. The findings corroborate previous research conducted by Näsi et al. (2015), which similarly found red-edge and near-infrared bands from a Fabry-Pérot Interferometer hyperspectral sensor to be significant to the early detection of bark beetle infestation.

In this research, the red-edge spectral bands were found to be highly efficient in distinguishing healthy and infested canopies under bark beetles green and red attack. This is because the red-edge region is susceptible to chlorophyll content changes, which decline at the initial stages of infestation, causing reflectance shift towards shorter wavelengths (Gitelson et al., 1994). Likewise, the NIR bands manifested significant reductions in reflectance in infested canopies, which matched structural weakening of foliar tissues as a result of bark beetle activity. As explained by Näsi et al. (2015), NIR reflectance is intimately linked with canopy architecture, and the present results affirm that NIR bands are very good indicators of canopies at the green attack stage. The relative significant of the SWIR bands in Sentinel-2 data indicates that this range is perhaps less suitable at identifying early bark beetle-induced physiological changes, particularly at the canopy scale. In conclusion the DESIS data delivered better subtle spectral differentiation between different bark beetles infestation phases, compared to Sentinel-2 because of its higher spectral resolution, especially in the red-edge and NIR spectral ranges.

4.4 Mapping Bark Beetles Green Attack Using the Random Forest Model

Taken a close look at the relative performance of the two RF models Model A, with both significant bands and vegetation indices, and Model B (see Figure 1) limited to only the significant bands, shows considerable disparity in classification performance between the Sentinel-2 and DESIS datasets. This disparity is not incidental but rather reflects fundamental differences associated with sensor design and input feature for the RF models.

Both models, in their first performances, had the ability to identify bark beetle green attack pixels across the study area (Figure 11 &12) although the extent of their performance was obviously defined by the sensor used and variability of input features. Model A, based on a large input feature set, performed better than Model B in all cases. DESIS achieved a classification accuracy of 47%, with 733 infested pixels correctly classified, compared to Sentinel-2's 41% (Table 5). These are suggestive of a good lead in integrating vegetation indices, particularly for Sentinel-2. Sentinel-2's broader spectral bands, while useful for coarse land cover mapping, lack the resolution to distinguish between subtle spectral differences during bark beetles green attack. The benefit of using vegetation indices here appears to be complementary to it coarse spectral resolution.

Moreover, the decrease in the proportion of pixels misclassified by DESIS (53%) in comparison to Sentinel-2 (59%) (Table 5) further supports the value of higher spectral resolution. Due to its capability to sense even less pronounced biochemical and physiological changes within the canopy, DESIS provides a more stable basis for successful early detection (Clark, 2018). This observation is supported by previous studies quoting the invaluable contribution hyperspectral data make towards the assessment of vegetation stress (Lu et al., 2019).

With regards to Model B, the contrast is even more pronounced. Here, DESIS achieved a very high accuracy rate of 46%, and the performance of Sentinel-2 decreased significantly to 9% (Table 6). Such a huge decline highlights the fundamental limitation of multispectral systems: when the input feature is limited, the low spectral resolution is ineffective in discriminating against the subtle spectral signatures that differentiate between healthy canopies and those under bark beetles stress. In contrast, DESIS with its large-scale spectral resolution preserves a great deal of discriminative power, even when the number of input features is lowered. These results are in line with the agreement that hyperspectral sensors are naturally more capable of noticing slight reflectance differences, especially during the initial stress in vegetation.

Temporal variations are worth considering. An eight-day offset between the DESIS and Sentinel-2 datasets adds an additional complexity. The vegetative dynamics, and particularly under the situation of repeated bark beetles infestation, can change radically during short time periods. Osińska-Skotak et al. (2019) also note that the timing of image acquisition plays significant role in determining classification accuracy in dynamic forest ecosystems. These temporal variations might have resulted in differences in detection efficacy, especially at the onset or transitional phases of bark beetle infestation.

Importantly, the benefit from adding vegetation indices was not equally beneficial to Sentinel-2. While DESIS had only marginal improvements with their inclusion, Sentinel-2's accuracy was greatly enhanced. This implies that for multispectral sensors, the derived indices are not simply additive but instrumental to overcoming spectral constraints and achieving physiological stress detection. Previous studies (Abdullah et al., 2018; Jamali et al., 2024) have acknowledge vegetation indices as a fundamental element to enhancing the early detection potential of multispectral imagery.

The analysis reaffirms the great potential of hyperspectral imagery i.e., the DESIS image spectroscopy in early bark beetle infestation detection. DESIS's high spectral resolution enables the capture of subtle canopy changes often not detectable by multispectral systems like Sentinel-2. Yet, optimal model performance is not solely reliant on sensor choice; careful feature selection and careful timing of image acquisition are still paramount.

4.6 Implications for Forest Management

It is important to detect the green attack stage early to minimize the damaging effects associated with bark beetle infestation and their spread to neighboring vulnerable spruce trees. The stage is an optimal intervention point since infestations when allowed to advance to the red attack stage tend to cause irreparable harm. From a forestry management perspective, early detection will enable more effective response actions, such as selective removal of trees or debarking, to manage outbreaks and minimize ecological and economic losses.

Traditional detection methods, such as ground surveys, although accurate, are hallmarked by intensive labor requirements, large time consumption, and are often impractical for large-scale forest monitoring. The outcome of this study supports the use of hyperspectral imaging as a complementary tool to conventional aerial surveys for operational forest monitoring, a perspective also highlighted by Abdullah et al. (2018). By providing detailed spectral data over large areas, hyperspectral data can help achieve reduced monitoring costs and improved early detection capabilities.

Furthermore, the detection of significant spectral bands in the DESIS and Sentinel-2 data provides an opportunity to create remote sensing indices specifically tailored for bark beetle infestation identification. Such indices could be formulated to capture subtle chlorophyll content changes and canopy structure changes related to early beetle activity stages, improving the accuracy and effectiveness of forest health monitoring.

4.7 Study Limitations and Future Research

While this study demonstrated promising results, several limitations should be acknowledged. First, due to time constraints, only the RF algorithm was employed for mapping bark beetle green infestations. Although RF is widely used for classification tasks, future research could benefit from testing and comparing multiple machine learning algorithms to identify the most effective approach for bark beetle detection.

identify the most effective approach for bark beetle detection.

Second, the DESIS sensor provides high spectral resolution imagery across the 400–1000 nm range, but it does not cover the shortwave infrared (SWIR) region (1000nm-2500nm). This limits its ability to capture some spectral signatures associated with vegetation stress. Future studies might consider using imaging spectroscopy missions with broader spectral coverage, such as PRISMA (PRecursore IperSpettrale della Missione Applicativa), EnMAP (Environmental Mapping and Analysis Program), or the upcoming CHIME (Copernicus Hyperspectral Imaging Mission for the Environment), to address this gap. Furthermore, although DESIS offers 235 narrow spectral bands, its spatial resolution of 30 meters limits its capacity to detect small early-stage infestation patches a limitation also noted by Shojanoori et al. (2016). In contrast, high-resolution multispectral sensors like PlanetScope and WorldView-3 offer much finer spatial resolution (up to 0.3–3 meters) but lack the spectral richness of hyperspectral sensors. To overcome these trade-offs, future research could explore data fusion techniques that integrate the spectral depth of DESIS with the spatial precision of high-resolution sensors. This fusion approach has been proposed by Gašparović (2018) to enhance detection accuracy and spatial detail in remote sensing applications. Lastly, this study compared DESIS and Sentinel-2 imagery, but the acquisition dates between the datasets did not fully align. For instance, the DESIS image was captured on April 10th, 2021, whereas the closest cloud-free Sentinel-2 image was from April 15th, 2021. These temporal differences may have introduced inconsistencies in the analysis. Additionally, while DESIS imagery was already pre-processed and free of clouds and atmospheric effects, Sentinel-2 imagery required substantial pre-processing, including cloud masking, which may have affected reflectance values in some areas. To improve the robustness of future analyses, efforts should be made to use imagery acquired on the same or near-identical dates and to apply harmonized preprocessing protocols across datasets.

5. CONCLUSION AND RECOMMENDATIONS

5.1 Conclusion

This study investigated the potential of DESIS image spectroscopy and Sentinel-2 data in detecting and mapping early-stage bark beetle infestations (green attack) at the canopy level in the Bavarian Forest National Park (BFNP). The research focused on the green attack phase, a critical stage where signs of infestation are not visible to the human eye, but biochemical and physiological changes in the canopy can be detected with high spectral resolution remote sensing data.

The main objectives of this research were to examine the spectral differences between healthy and infested Norway spruce canopies, to identify the spectral bands significant for detecting the green attack phase, and to explore the potential of spectral bands from DESIS image spectroscopy and Sentinel-2 for mapping bark beetle green attacks.

Key findings include the research ability to distinguish spectral characteristics between healthy and infested canopies across various infestation phases, particularly during the green and red attack phases. During these phases the infested canopies exhibit higher reflectance in visible regions and lower reflectance in the NIR region across all the two datasets. The study also established a relationship between bark beetle infestation stages and the REP in both datasets, as the bark beetles infestation progresses the REP shift towards the shorter wavelengths except in the case of green attack. Furthermore, using a one-way ANOVA test, the research identified spectral bands in both datasets that significantly differentiate healthy and infested canopies during the green attack phase, these bands were basically located in the red edge region and NIR for the two datasets, corroborating existing knowledge in literature.

Additionally, the study was able, to some extent, map bark beetle infestations using DESIS image spectroscopy and Sentinel-2 data. Although the number of pixels identified as green attack was fewer compared to reference data from aerial photography, the research demonstrated the feasibility of mapping early-stage infestations at the canopy level. These findings provide a foundation for future studies to improve detection accuracy by developing advanced machine learning algorithms.

Moreover, the approach used in this study can be replicated globally and is not limited to bark beetles infestation detection alone . The methodology used in this research can also be applied to detect and monitor other pests or disease damage in forests and food crops.

In summary, this study contributes to understanding the role of satellite-based hyperspectral and multispectral data in monitoring bark beetle infestations at the canopy level and proposes an effective methodology for future research in forest ecology. The findings indicate that satellite-based hyperspectral data (DESIS) is more cost-effective for detecting early-stage bark beetle infestations at the canopy level compared to multispectral data such as Sentinel-2. Consequently, this research has significant implications for monitoring, preparedness, and management strategies related to bark beetle infestations.

5.2 Recommendations

Based on the limitations of this study, future research on this topic should consider addressing the following issues to improve the early detection and mapping of green attack bark beetle infestations at the canopy level

I. Although DESIS image spectroscopy data has high spectral resolution, its moderate spatial resolution makes it difficult to detect infestation patches smaller than 900 m^2. Future research could explore data fusion methods by combining DESIS data with higher-resolution imagery such as PlanetScope or WorldView-3 to improve detection of infestations.

II. Additionally, DESIS provides high spectral resolution hyperspectral data, it only covers the 400–1000 nm range, missing the SWIR region. Other satellite-based imaging spectroscopy missions such as PRISMA, EnMAP, and the upcoming CHIME offer more comprehensive spectral coverage, which feature studies may consider

III. Only the RF algorithm was used in this research to map bark beetle green infestations due to time constraints. Future studies may consider incorporating other machine learning algorithms such as Support Vector Machines or Neural Networks.

6 ETHICAL CONSIDERATIONS.

Since this study does not involve gathering sensitive or personal data, there are not any immediate ethical issues. The main objective of this study is to use DESIS image spectroscopy data and Sentinel-2 data to map bark beetles infestations. The data used in this study are secondary sources of data, which were obtained from BFNP, DLR and Copernicus hub which have been properly cited. However, all the legislation and regulations of BFNP, DLR, ESA concerning handling of data were strictly followed.

7. LIST OF REFERENCES

Abdullah, H., Darvishzadeh, R., Skidmore, A. K., Groen, T. A., & Heurich, M. (2018). European spruce bark beetle (Ips typographus, L.) green attack affects foliar reflectance and biochemical properties. *International Journal of Applied Earth Observation and Geoinformation*, 64, 199–209. https://doi.org/10.1016/j.jag.2017.06.009

Abdullah, H., Skidmore, A. K., Darvishzadeh, R., & Heurich, M. (2019). Timing of red-edge and shortwave infrared reflectance critical for early stress detection induced by bark beetle (Ips typographus, L.) attack. *International Journal of Applied Earth Observation and Geoinformation,* 82, 101900. https://doi.org/10.1016/j.jag.2019.101900

Banninger, C. (1990). Fluorescence line imager measured "red edge shifts" in a metal-stressed Norway spruce forest and their relationship to canopy biochemical and morphological changes Proceedings of SPIE, *the International Society for Optical Engineering/Proceedings of SPIE*, 1298, 234–243. https://doi.org/10.1117/12.21357

Bárta, V., Hanuš, J., Dobrovolný, L., & Homolová, L. (2022). Comparison of field survey and remote sensing techniques for detection of bark beetle-infested trees. *Forest Ecology and Management*, *506*, 119984. https://doi.org/10.1016/j.foreco.2021.119984

Beamish, A., Coops, N., Chabrillat, S., & Heim, B. (2017). A phenological approach to spectral differentiation of Low-Arctic Tundra vegetation communities, North Slope, Alaska. *Remote Sensing*, 9(11), 1200. https://doi.org/10.3390/rs9111200

Bonan, G. B. (2008). Forests and climate change: forcings, feedbacks, and the climate benefits of forests. Science, 320(5882), 1444–1449. https://doi.org/10.1126/science.1155121

Boser, B. E., Guyon, I. M., & Vapnik, V. N. (1992). A training algorithm for optimal margin classifiers. A Training Algorithm for Optimal Margin Classifiers, 144–152. https://doi.org/10.1145/130385.130401

Breiman, L. (2001). Random forests. Machine Learning, 45(1), 5-32. https://doi.org/10.1023/A:1010933404324

Carter, G. A., & Knapp, A. K. (2001). Leaf optical properties in higher plants: linking spectral characteristics to stress and chlorophyll concentration. *American Journal of Botany*, *88*(4), 677–684. https://doi.org/10.2307/2657068

Carter, G. A. (1993). Responses of leaf spectral reflectance to plant stress. *American Journal of Botany*, *80*(3), 239. https://doi.org/10.2307/2445346

Clark, M. L. (2018). Identification of canopy species in tropical forests using hyperspectral data. In *CRC Press eBooks* (pp. 211–232). https://doi.org/10.1201/9780429431180-7

Clevers, J. G. P. W., & Gitelson, A. A. (2013). Remote Sensing estimation of crop and grass chlorophyll and nitrogen content using red-edge bands on Sentinel-2 and the REIP concept. *International Journal of Applied Earth Observation and Geoinformation,* 23, 344-351. https://doi.org/10.1016/j.jag.2012.10.008

Coops, N. C., Wulder, M. A., Culvenor, D. S., & St-Onge, B. (2004). Comparison of forest attributes extracted from fine spatial resolution multispectral and lidar data. *Canadian Journal of Remote Sensing*, 30(6), 855–866. https://doi.org/10.5589/m04-045

Cortes, C., & Vapnik, V. (1995). Support-vector networks. Machine Learning, 20(3), 273–297. https://doi.org/10.1007/bf00994018

Darvishzadeh, R., Ali, A.M., Skidmore, A.K., Abdullah, H., Heurich, M., & Marc, P. (2020). Detecting bark beetle infestation using plants canopy chlorophyll content retrieved from remote sensing data.

Dean, K.G., Kodama, Y., & Wendler, G. (1986). Comparison of leaf and canopy reflectance of subarctic forests. Photogrammetric Engineering and Remote Sensing, 52, 809-811.

Fahse, L., & Heurich, M. (2011). Simulation and analysis of outbreaks of bark beetle infestations and their management at the stand level. Ecological Modelling, 222(11), 1833–1846. https://doi.org/10.1016/j.ecolmodel.2011.03.014

Felicijan, M., Novak, M., Kraševec, N., & Krajnc, A. U. (2015). Antioxidant defences of Norway spruce bark against bark beetles and its associated blue-stain fungus. *Agricultura*, *12*(1–2), 9–18. https://doi.org/10.1515/agricultura-2016-0002

Fernández, C. I., Leblon, B., Haddadi, A., Wang, K., & Wang, J. (2020). Potato late blight detection at the leaf and canopy levels based in the red and Red-Edge spectral regions. *Remote Sensing*, 12(8), 1292. https://doi.org/10.3390/rs12081292

Gao, B. (1996). NDWI, A normalized difference water index for remote sensing of vegetation liquid water from space. *Remote Sensing of Environment*, 58(3), 257–266. Https://doi.org/10.1016/s0034-4257(96)00067-3

Gašparović, M., Medak, D., Pilaš, I., Jurjević, L., & Balenović, I. (2018b). Fusion Of Sentinel-2 And Planetscope Imagery For Vegetation Detection And Monitoring. *the International Archives of the Photogrammetry, Remote Sensing and Spatial Information Sciences/International Archives of the Photogrammetry, Remote Sensing and Spatial Information Sciences*, *XLII–1*, 155–160. https://doi.org/10.5194/isprs-archives-xlii-1-155-2018

Gitelson, A., & Merzlyak, M. N. (1994). Quantitative estimation of chlorophyll-a using reflectance spectra: Experiments with autumn chestnut and maple leaves. *Journal of Photochemistry and Photobiology B Biology*, 22(3), 247–252. https://doi.org/10.1016/1011-1344(93)06963-4

Gitelson, A. A., Kaufman, Y. J., & Merzlyak, M. N. (1996). Use of a green channel in remote sensing of global vegetation from EOS-MODIS. *Remote Sensing of Environment,* 58(3), 289–298. https://doi.org/10.1016/s0034-4257(96)00072-7

Gong, N. P., Pu, N. R., Biging, G., & Larrieu. (2003). Estimation of forest leaf area index using vegetation indices derived from hyperion hyperspectral data. *IEEE Transactions on Geoscience and Remote Sensing*, 41(6), 1355–1362. https://doi.org/10.1109/tgrs.2003.812910

Guyot, G., & Baret, F. (1988). *Utilisation de la haute résolution spectrale pour suivre l'état des couverts végétaux*. In Proceedings of the 4th International Colloquium on Spectral Signatures of Objects in Remote Sensing (pp. 279–286). Aussois, France: ESA Publication SP-287.

Haagsma, M., Page, G., Johnson, J., Still, C., Waring, K., Sniezko, R., & Selker, J. (2020). Is more data better? A comparison of multi- and hyperspectral imaging in phenotyping. NA. Https://doi.org/10.5194/egusphere-egu2020-10673

Hais, M., Wild, J., Berec, L., Brůna, J., Kennedy, R., Braaten, J., & Brož, Z. (2016). Landsat Imagery Spectral Trajectories—Important variables for spatially predicting the risks of bark beetle disturbance. *Remote Sensing*, *8*(8), 687. https://doi.org/10.3390/rs8080687

Heurich, M. (2009). Progress of forest regeneration after a large-scale Ips typographus outbreak in the subalpine Picea abies forests of the Bavarian Forest National Park. *Silva Gabreta*, *15*. https://weevil.myspecies.info/progress-forest-regeneration-after-large-scale-ips-typographus-outbreak-subalpine-picea-abies-forest

Heurich, M., Beudert, B., Rall, H., & Křenová, Z. (2010). National Parks as model regions for Interdisciplinary Long-Term Ecological research: The Bavarian Forest and Šumavá National Parks Underway to Transboundary Ecosystem research. In *Springer eBooks* (pp. 327–344). https://doi.org/10.1007/978-90-481-8782-9_23

Hicke, J. A., Allen, C. D., Desai, A. R., Dietze, M. C., Hall, R. J., Ted Hogg, E. H., ... & Luo, Y. (2012). Effects of biotic disturbances on forest carbon cycling in the United States and Canada. *Global Change Biology*, 18(1), 7-34. https://doi.org/10.1111/j.1365-2486.2011.02543.x

Hlásny, T., & Turčáni, M. (2013). Persisting bark beetle outbreak indicates the unsustainability of secondary Norway spruce forests: Case study from Central Europe. *Annals of Forest Science*, 70(4), 481–491. https://doi.org/10.1007/s13595-013-0279-7

Hlásny, T., König, L., Krokene, P., Lindner, M., Montagné-Huck, C., Müller, J., Qin, H., Raffa, K. F., Schelhaas, M. J., Svoboda, M., Viiri, H., & Seidl, R. (2021). Bark beetle outbreaks in Europe: State of knowledge and ways forward for management. *Current Forestry Reports,* 7, 138–165. https://doi.org/10.1007/s40725-021-00142-x

Hellwig, F. M., Stelmaszczuk-Górska, M. A., Dubois, C., Wolsza, M., Truckenbrodt, S. C., Sagichewski, H., Chmara, S., Bannehr, L., Lausch, A., & Schmullius, C. (2021). Mapping European spruce bark beetle infestation at its early phase using Gyrocopter-Mounted hyperspectral data and field measurements. *Remote Sensing*, 13(22), 4659. https://doi.org/10.3390/rs13224659

Huo, L., Lindberg, E., Bohlin, J., & Persson, H. J. (2023). Assessing the detectability of European spruce bark beetle green attack in multispectral drone images with high spatial- and temporal resolutions. Remote Sensing of Environment, 287, 113484. https://doi.org/10.1016/j.rse.2023.113484

Huo, L., Lindberg, E., Fransson, J. E., & Persson, H. J. (2022). Comparing Spectral Differences Between Healthy and Early Infested Spruce Forests Caused by Bark Beetle Attacks using Satellite Images. *IGARSS 2022 - 2022 IEEE International Geoscience and Remote Sensing Symposium*, 7709–7712. https://doi.org/10.1109/igarss46834.2022.9883420

Jamali, S., Olsson, P., Müller, M., & Ghorbanian, A. (2024). Kernel-Based Early Detection of Forest bark beetle attack using vegetation indices Time Series of Sentinel-2. *IEEE Journal* *of Selected Topics in Applied Earth Observations and Remote Sensing*, 17, 12868–12877. https://doi.org/10.1109/jstars.2024.3425795

Jung, A., Kardeván, P., & Tőkei, L. (2006). Hyperspectral technology in vegetation analysis. Progress in Agricultural Engineering Sciences, 2(1), 95–117. https://doi.org/10.1556/progress.2.2006.1.5

Kamusoko, C. (2019). Improving image classification. *In Springer geography* (pp. 155–181). https://doi.org/10.1007/978-981-13-8012-9_5

Kautz, M., Feurer, J., & Adler, P. (2024). Early detection of bark beetle (Ips typographus) infestations by remote sensing – A critical review of recent research. *Forest Ecology and Management*, *556*, 121595. https://doi.org/10.1016/j.foreco.2023.121595

Kautz, M., Peter, F. J., Harms, L., Kammen, S., & Delb, H. (2023). Patterns, drivers, and detectability of infestation symptoms following attacks by the European spruce bark beetle. Journal of Pest Science, 96, 403–414. https://doi.org/10.1007/s10340-022-01490-8

Kim, T. K. (2017). Understanding one-way ANOVA using conceptual figures. *Korean journal of anesthesiology*, 70(1), 22. references for understanding the anova test

Krstajic, D.; Buturovic, L.J.; Leahy, D.E.; Thomas, S. Cross-Validation Pitfalls When Selecting and Assessing Regression and Classification Models. *J. Cheminform*. 2014, 6, 1–15, doi:10.1186/1758-2946-6-10.

Lausch, A., Erasmi, S., King, D. J., Magdon, P., & Heurich, M. (2016). Understanding Forest Health with Remote Sensing -Part I—A Review of Spectral Traits, Processes and Remote-Sensing Characteristics. *Remote Sensing*, *8*(12), 1029. https://doi.org/10.3390/rs8121029

Lausch, A., Heurich, M., & Fahse, L. (2013). Spatio-temporal infestation patterns of Ips typographus (L.) in the Bavarian Forest National Park, Germany. *Ecological Indicators*, 31, 73–81. https://doi.org/10.1016/j.ecolind.2013.01.034

Luyssaert, S., Schulze, E.-., Börner, A., Knohl, A., Hessenmöller, D., Law, B. E., Ciais, P., & Grace, J. (2008). Old-growth forests as global carbon sinks. Nature, 455(7210), 213–215. https://doi.org/10.1038/nature07276

Lu, B., He, Y., & Dao, P. D. (2019). Comparing the performance of multispectral and hyperspectral images for estimating vegetation properties. *IEEE Journal of Selected Topics in Applied Earth Observations and Remote Sensing*, *12*(6), 1784–1797. https://doi.org/10.1109/jstars.2019.2910558

Marvasti-Zadeh, S. M., Goodsman, D., Ray, N., & Erbilgin, N. (2023). Early detection of bark beetle attack using remote sensing and Machine Learning: A review. ACM Computing Surveys, 56(4), 1–40. https://doi.org/10.1145/3625387

Marx, A. (2010). Erkennung von Borkenkäferbefall in Fichtenreinbeständen mit multitemporalen Rapid-Eye-Satellitenbildern und Data-Mining-Techniken. Photogrammetrie, Fernerkundung, *Geoinformation* (PFG), 4, 243–252. https://doi.org/10.1127/1432-8364/2010/0055

Masaitis, G., Mozgeris, G., & Augustaitis, A. (2013). Spectral reflectance properties of healthy and stressed coniferous trees. iForest - Biogeosciences and Forestry, 6(1), 30–36. https://doi.org/10.3832/ifor0709-006

Mayer, M., Müller, M., Metzler, D., & Martin, M. (2010). Regional economic impact of Bavarian Forest National Park. UZH. https://doi.org/10.5167/uzh-78803

Morin, M., Lawrence, R., Repasky, K., Sterling, T., McCann, C., & Powell, S. (2017). Agreement analysis and spatial sensitivity of multispectral and hyperspectral sensors in detecting vegetation stress at management scales. *Journal of Applied Remote Sensing*, *11*(04), 1. https://doi.org/10.1117/1.jrs.11.046025.

Morris, J. L., Cottrell, S., Fettig, C. J., DeRose, R. J., Mattor, K. M., Carter, V. A., ... & Seybold, S. J. (2018). Bark beetles as agents of change in social-ecological systems. *Frontiers in Ecology and the Environment*, 16(S1), S34–S43. https://doi.org/10.1002/fee.1754

Mutanga, O., & Skidmore, A. K. (2004). Narrow band vegetation indices overcome the saturation problem in biomass estimation. International Journal of Remote Sensing, 25(19), 3999–4014. https://doi.org/10.1080/01431160310001654923

Murphy, R. J. (1995). The effects of surficial vegetation cover on mineral absorption feature parameters. *International Journal of Remote Sensing*, 16(12), 2153–2164. https://doi.org/10.1080/01431169508954548

Näsi, R., Honkavaara, E., Lyytikäinen-Saarenmaa, P., Blomqvist, M., Litkey, P., Hakala, T., ... & Holopainen, M. (2015). Using UAV-Based Photogrammetry and Hyperspectral Imaging for Mapping Bark Beetle Damage at Tree-Level. *Remote Sensing*, 7(11), 15467-15493. https://doi.org/10.3390/rs71115467

Netherer, S., & Schopf, A. (2010). Potential effects of climate change on insect herbivores in European forests—general aspects and the pine processionary moth as specific example. *Forest Ecology and Management*, 259(4), 831–838. https://doi.org/10.1016/j.foreco.2009.07.034

Osińska-Skotak, K., Radecka, A., Piórkowski, H., Michalska-Hejduk, D., Kopeć, D., Tokarska-Guzik, B., Ostrowski, W., Kania, A., & Niedzielko, J. (2019). Mapping succession in Non-Forest habitats by means of remote sensing: Is the data acquisition time critical for species discrimination*? Remote Sensing*, 11(22), 2629. https://doi.org/10.3390/rs11222629

Pause, M., Schweitzer, C., Rosenthal, M., Keuck, V., Bumberger, J., Dietrich, P., Heurich, M., Jung, A., & Lausch, A. (2016). *In Situ*/Remote Sensing Integration to Assess Forest Health—A Review. *Remote Sensing*, *8*(6), 471. https://doi.org/10.3390/rs8060471

Pu, R., Gong, P., Biging, G. S., & Larrieu, M. R. (2003). Extraction of red edge optical parameters from Hyperion data for estimation of forest leaf area index. *IEEE Transactions on Geoscience and Remote Sensing,* 41(4), 916−921. for polynomial fitting

Qi, J., Chehbouni, A., Huete, A., Kerr, Y., & Sorooshian, S. (1994). A modified soil adjusted vegetation index. Remote Sensing of Environment, 48(2), 119–126. https://doi.org/10.1016/0034-4257(94)90134-1

Schmidt, M., & Overbeck, G. E. (2012). Modelling infestation risk of Norway spruce by Ips typographus (L.) in the Lower Saxon Harz Mountains (Germany). *Forest Ecology and Management*, 266, 115–125. https://doi.org/10.1016/j.foreco.2011.11.011

Siegert, C., Clay, N., Pace, K., Vissa, S., Hofstetter, R. W., Leverón, O., & Riggins, J. J. (2024). Bark beetle-driven community and biogeochemical impacts in forest ecosystems: a review. *Annals of the Entomological Society of America*, *117*(3), 163–183. https://doi.org/10.1093/aesa/saae009

Shojanoori, R., & Shafri, H. (2016). Review on the use of remote sensing for Urban Forest Monitoring. *Arboriculture & Urban Forestry*, *42*(6). https://doi.org/10.48044/jauf.2016.034.

Seidl, R., Schelhaas, M. J., Rammer, W., & Verkerk, P. J. (2016). Increasing forest disturbances in Europe and their impact on carbon storage. *Nature Climate Change*, 6(9), 806–810. https://doi.org/10.1038/nclimate2318

Simmer, C, & Gerstl, S A.W. (1985). Influence of the atmosphere on remotely sensed reflection from vegetation surfaces. https://doi.org/10.1364/ORS.1985.WC18

Somers, B., & Asner, G. P. (2013). Hyperspectral time series analysis of native and invasive species in Hawaiian rainforests. *Remote Sensing*, 5(11), 5143–5160. https://doi.org/10.3390/rs4092510

Stemberk, J. (2020). ECONOMIC BENEFITS OF ŠUMAVA NATIONAL PARK. International Scientific Conference ITEMA. Recent Advances in Information Technology, Tourism, Economics, Management and Agriculture, 73–81. https://doi.org/10.31410/itema.2020.73

Story, M., & Congalton, R. G. (1986). Accuracy assessment: a user's perspective. *Photogrammetric Engineering and remote sensing*, 52(3), 397-399. references for producer and user accuracy

Ustin, S. L., & Gamon, J. A. (2010). Remote sensing of plant functional types. New Phytologist, 186(4), 795-816. https://doi.org/10.1111/j.1469-8137.2010.03284.x

Vege, M., & Hofstetter, R. W. (2015). Bark Beetles: Biology and Ecology of Native and Invasive Species. Academic Press.

Velichkova, K., & Krezhova, D. (2019). Extraction of the red edge position from hyperspectral reflectance data for plant stress monitoring. AIP Conference Proceedings. https://doi.org/10.1063/1.5091303

Waldhäuser Climate Station, 2021 Access from Bavarian Forest National Park Climate Monitoring databased.

Xu, H. (2006). Modification of normalised difference water index (NDWI) to enhance open water features in remotely sensed imagery. *International Journal of Remote Sensing*, 27(14), 3025–3033. Https://doi.org/10.1080/01431160600589179

Yoder, B. J., & Waring, R. H. (1994). The normalized difference vegetation index of small Douglas-fir canopies with varying chlorophyll concentrations. *Remote Sensing of Environment*, *49*(1), 81–91. https://doi.org/10.1016/0034-4257(94)90061-2

Zarco-Tejada, P. J., Camino, C., Beck, P. S. A., Calderon, R., Hornero, A., Hernández-Clemente, R., ... & North, P. R. J. (2018). Previsual symptoms of Xylella fastidiosa infection revealed in spectral plant-trait alterations. *Nature Plants*, 4(7), 432-439. https://doi.org/10.1038/s41477-018-0189-7

AI Statement

During the preparation of this thesis, I used ChatGPT only to revise the texts to avoid grammatical errors . After using the tool, I reviewed and edited the content as needed and takes full responsibility of the content of the work

8 APPENDIX

8.1 Data Management Plan (DMP)

8.1.1 Data collection

Table APP1. Research data collection.

Data type	Data format	File format	Contains personal data (yes/no). if yes which?	is the right to the data claimed by a third party (yes/n0). if yes, which third party?
DESIS hyperspectral data (April, June and August) 2021	Satellite Imagery	.tiff/.h5	No	Y - Claimed by the German Aerospace Center (DLR)
Beetle Infestation Data (2021)	Vector (Polygon)	shp, .dbf, .shx, .prj	No	Y - Claimed by Bavarian Forest Authority
Bavarian Forest Shapefile	Vector (Polygon)	shp, .dbf, .shx, .prj	No	Y - Claimed by Bavarian Forest Authority
Sentinel-2	Raster	JPEG 2000	No	Y- Claimed by ESA
Land Use Land Cover	Vector (Polygon)	shp, .dbf, .shx, .prj	No	Y- Claimed by Bavarian Forest Authority
Healthy stands (2016)	Polygon (points)	shp, .dbf, .shx, .prj	No	Y- Field campaign in 2016

8.1.2 Data Organizing and Documenting

Folder Structure:

- **Main Folder:** Msc_Thesis_Dataset 2025
- **Subfolders:**
    - **Hyperspectral_Data**
        - DESIS_2021 April
        - DESIS_ 2021 June
        - DESIS_2021 August
        -
    - **Multispectral_data**
        - Sentinel-2_2021 April
        - Sentinel-2_2021 June
        - Sentinel-2_2021August
    - **Infestation_Data-2021**
        - Reference infestation data_2021
        -

- **Boundary_Shapefile_Data**
    - BavarianForest_Shapefile
- **Land Use Land Cover**

    - LULC

- **Heathy stands 2016**

    - Health spruce stands 2016

- **Results**
    - Bark beetles infestation maps
    - Statistics
    - Spectral curves
- **Documentation**
    - Metadata
    - Readme_Files

8. 1.3 File Naming Convention:

- DESIS hyperspectral data for the Bavarian Forest: DESIS_BavarianForest_2021_April_Hyperspectral_v1.0.tiff
- DESIS_BavarianForest_2021_June_Hyperspectral_v1.0.tiff
- DESIS_BavarianForest_2021_August_Hyperspectral_v1.0.tif bf
- Sentinel-2_BavarianForest_2021_August_Multispectral_v1.0.tiff
- Sentinel-2_BavarianForest_2021_June_Multispectral_v1.0.tiff
- Sentinel-2_BavarianForest_2021_April_Multispectral_v1.0.tiff
- Beetle infestation data shapefile: BeetleInfestation_BavarianForest__v1.0.shp
- Heathy spruce stands_2016_v1.0.shp
- LULC_2016_v1.0.shp
- Results of spectral curves for beetle-infested areas: Spectralcurves_BavarianForest_Infested_v1.0.tiff

8.1.4 Data Storage and Sharing

- **Main Storage:**
    - All primary data will be stored in a secure cloud storage solution provided by University of Twente which meets the necessary data security regulations.
- **Backup and Security Measures:**
    - Data will be backed up on encrypted external hard drives and a secondary secure cloud service (personal google drive)to prevent data loss.
    - Access to the data will be limited to authorized project members.

- Data will be encrypted both in transit and at rest. Additionally, sensitive geographic boundaries will be pseudonymized to prevent unauthorized use.

- **Data Sharing:**
  - Data will be shared with academic collaborators and made available to the wider research community through an institutional repository. Access will be restricted according to the third-party agreements with the German Aerospace Center and the Bavarian Forest Authority.

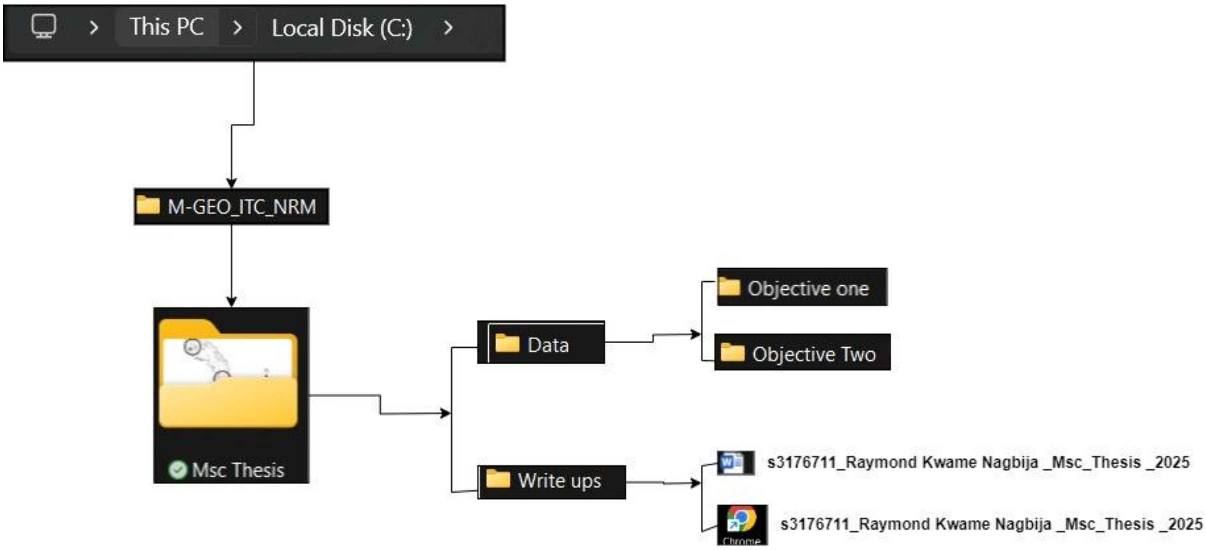

Figure APP1: Data storage and organization

7.1.5 Data Archiving

Table APP2: Data Archive Strategy

Data type	Data format for preservation	Can be made. Publicly available	Contains personal data (yes/no). if yes, which?	Restricted access + reason
DESIS hyperspectral data (April, June and August) 2021	Satellite Imagery	No	No	Yes, restricted by DRL licensing

Beetle Infestation Data (2021)	Vector (polygon)	No	No	Yes, restricted BFNP authorities
Bavarian Forest Shapefile	Vector (Polygon)	No	No	Yes, restricted by BFNP authorities
Sentinel-2	Raster	Yes	No	No open access
Healthy stand 2016	Vector (Points)	No	No	N/A
LULC	Vector (polygons)	No	No	Yes, restricted BFNP authorities

7.2 Other Figures

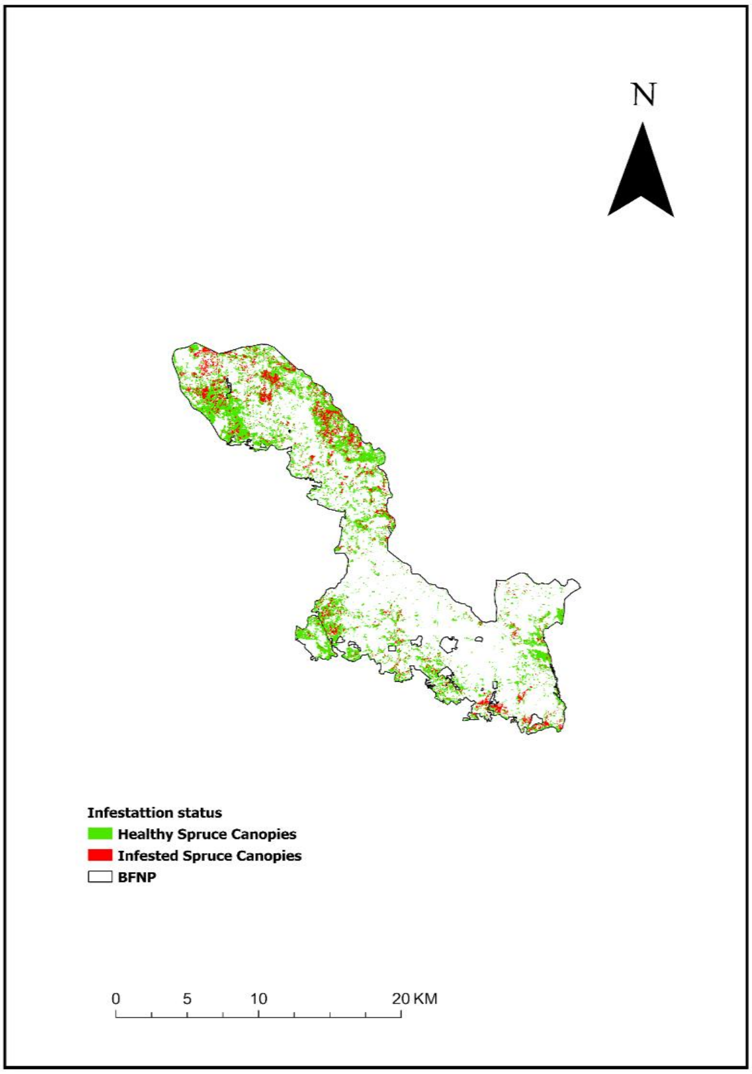

Figure APP3: Random Forest classification of bark beetles green attack using DESIS data (Significant bands only)

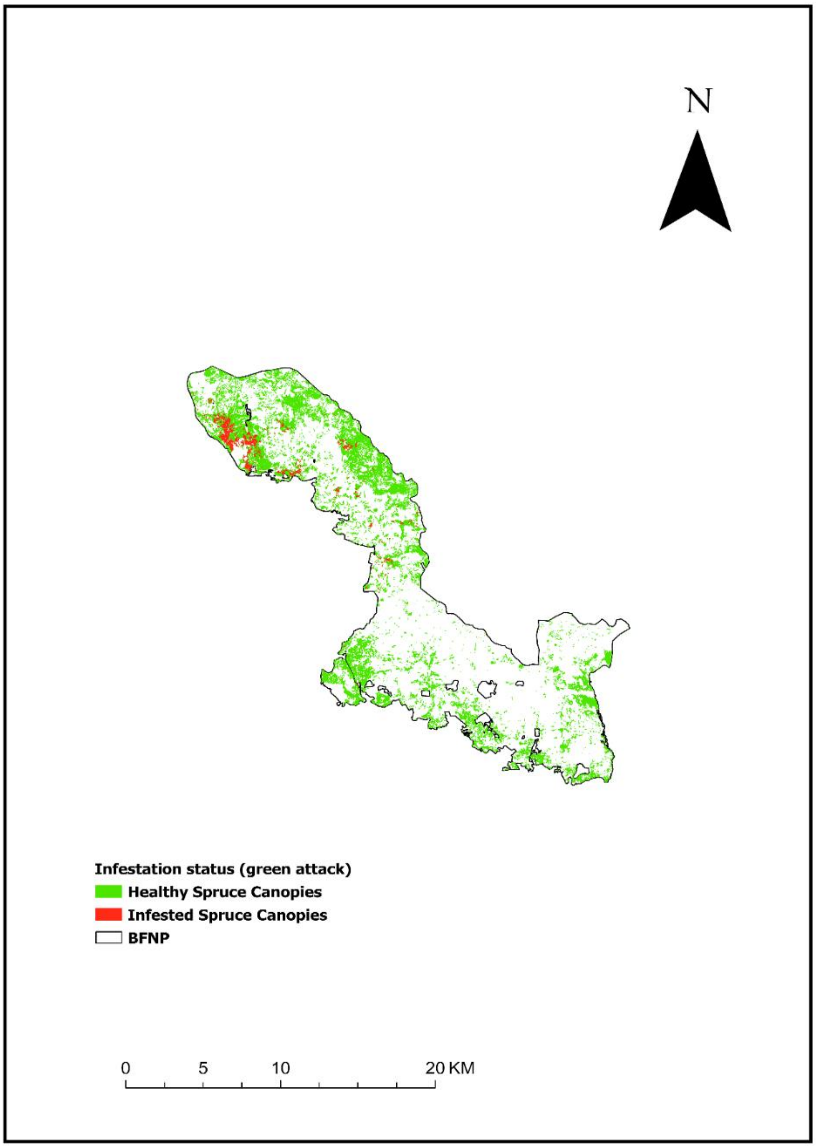

Figure APP4: Random Forest classification of bark beetles green attack using Sentinel-2 data (Significant bands only)

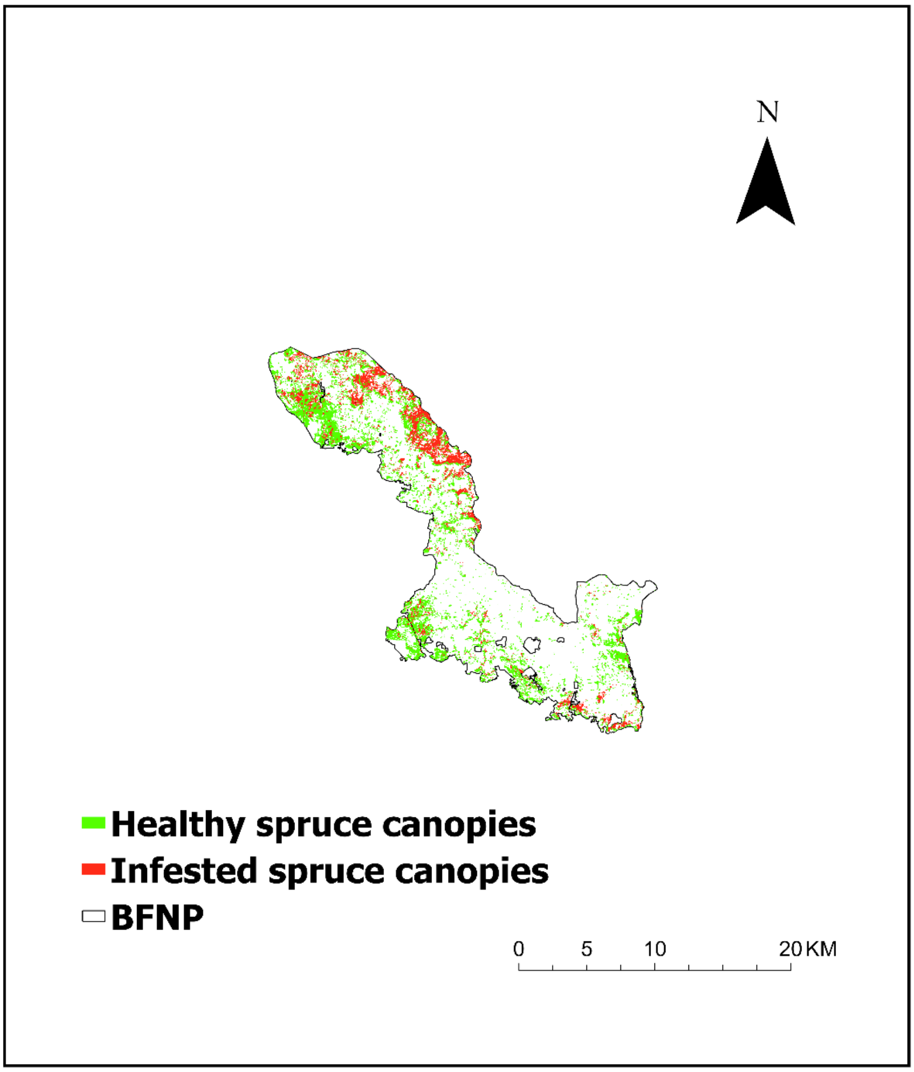

Figure APP5 : Random Forest classification of bark beetles green attack using Sentinel-2 data (Significant bands and vegetation indices)

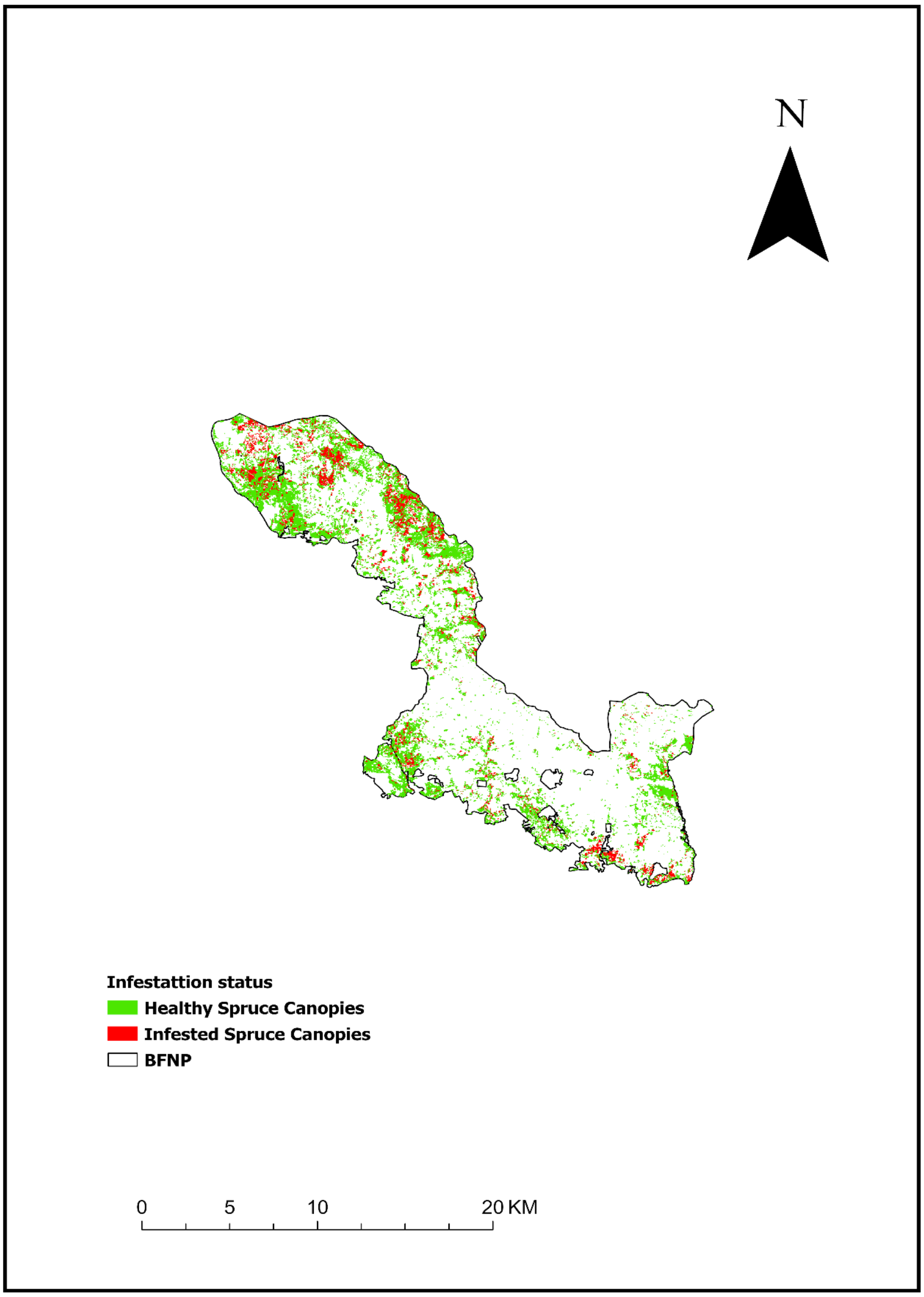

Figure APP6 : Random Forest classification of bark beetles green attack using DESIS data (Significant bands and vegetation indices)

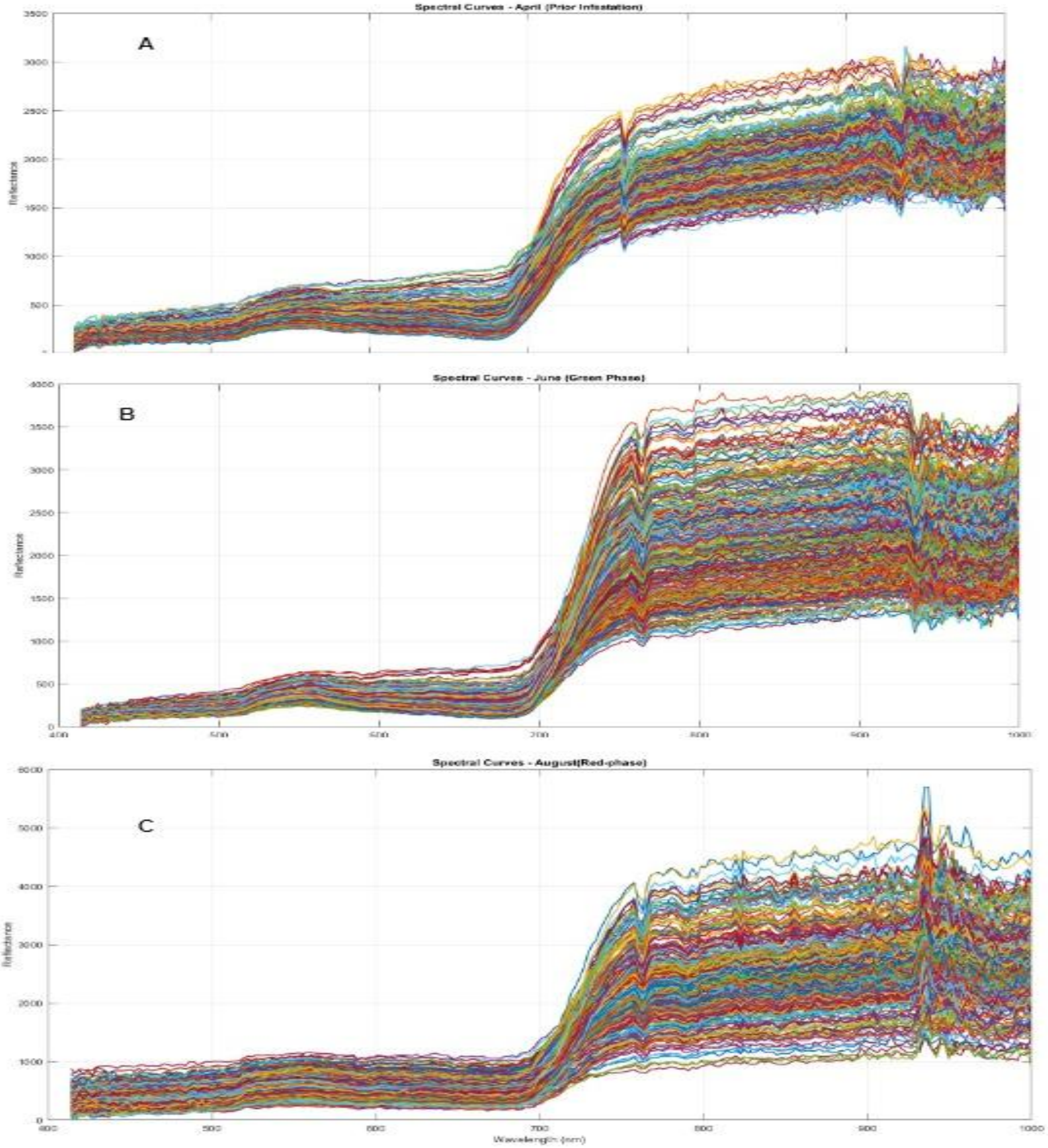

Figure APP7: Reflectance of DESIS image spectroscopy data. A prior to infestation , B Green attack and C red attack

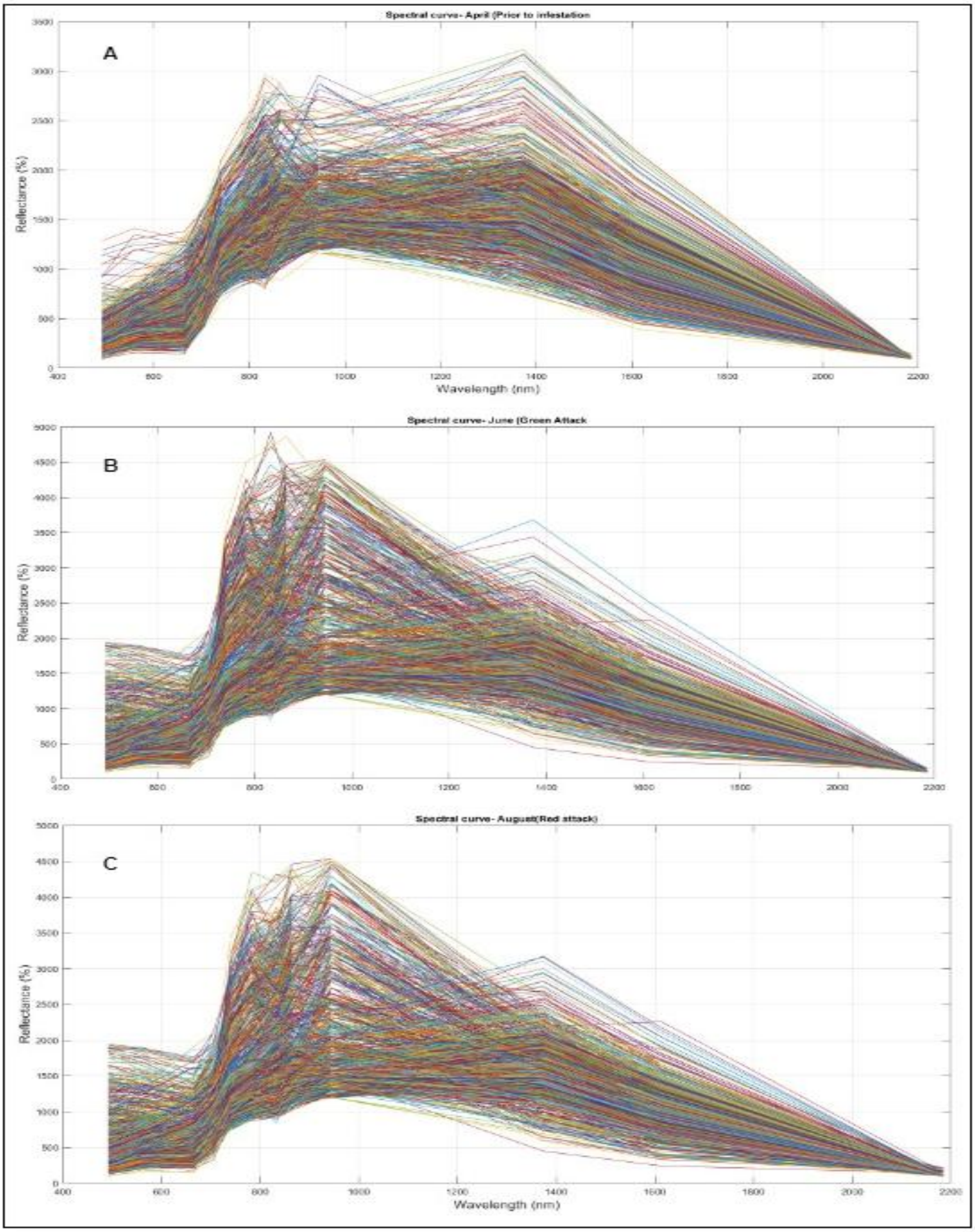

Figure APP7: Reflectance of Sentinel-2 data. A prior to infestation , B Green attack and C red attack

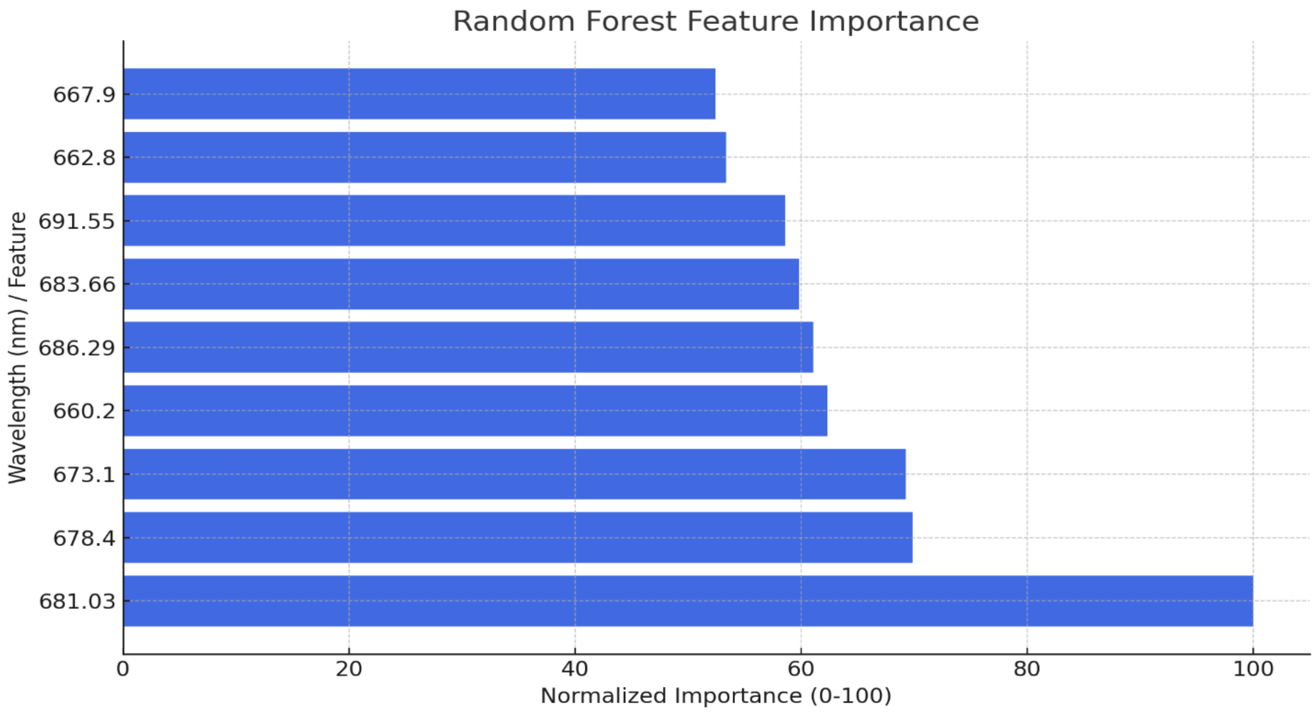

Figure APP8: RF feature importance for DESIS Model A (Vegetation Indices and Significant bands), the graph only considered features with at least 50% contribution to the classification process

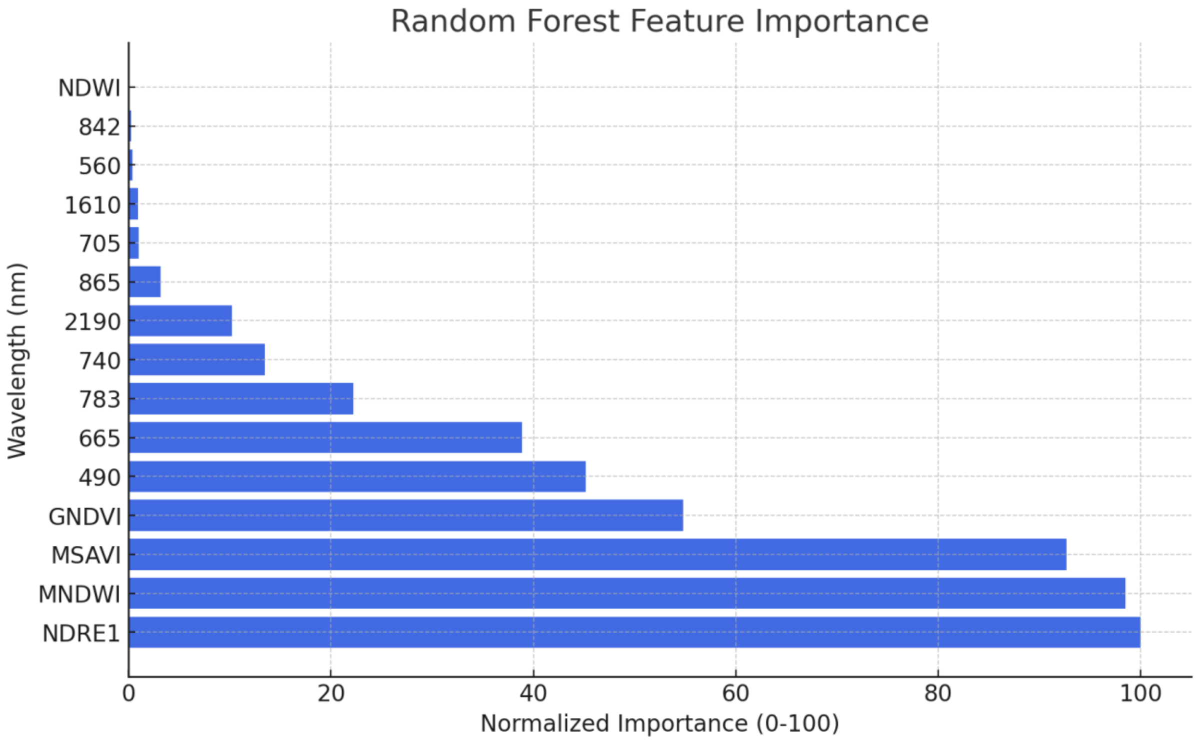

Figure 13: RF feature importance for Sentinel-2 Model A (Vegetation Indices and Significant bands).

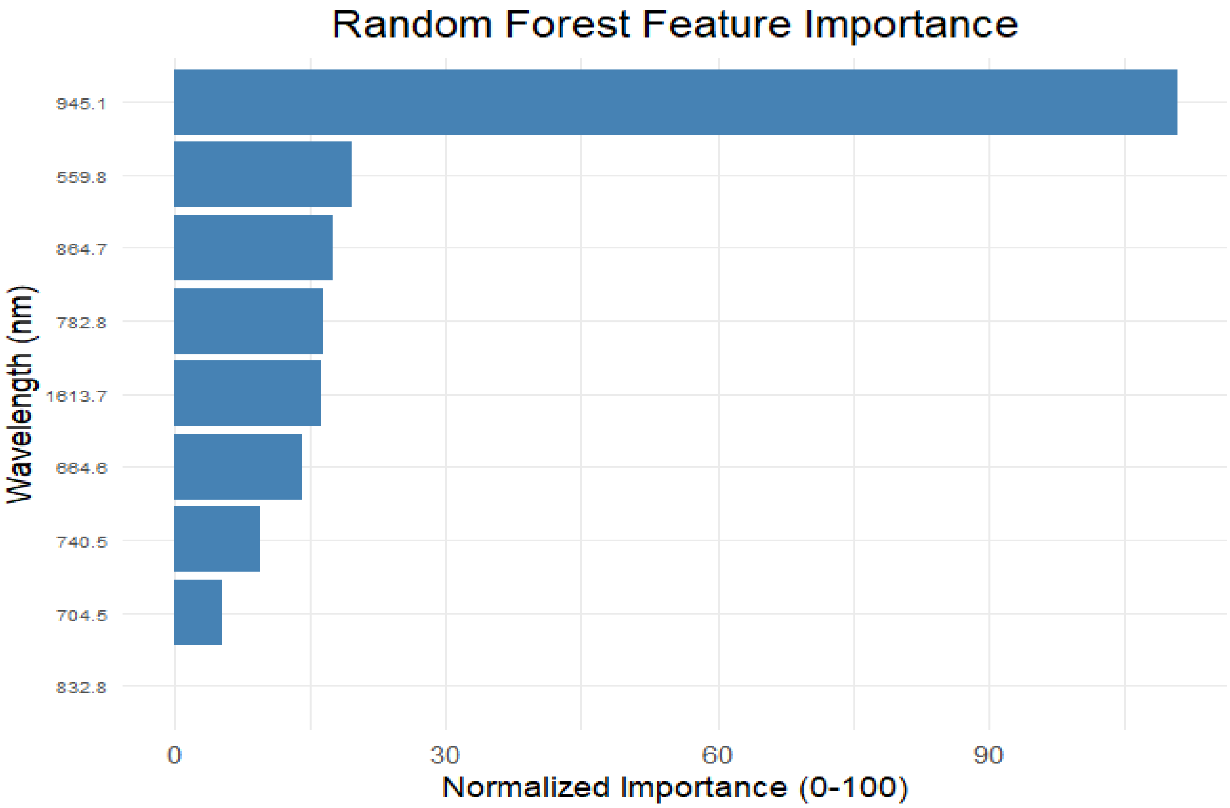

Figure APP9 : RF feature importance for Sentinel-2 Model B (Only significant bands), Only bands with at least 50% contribution were included

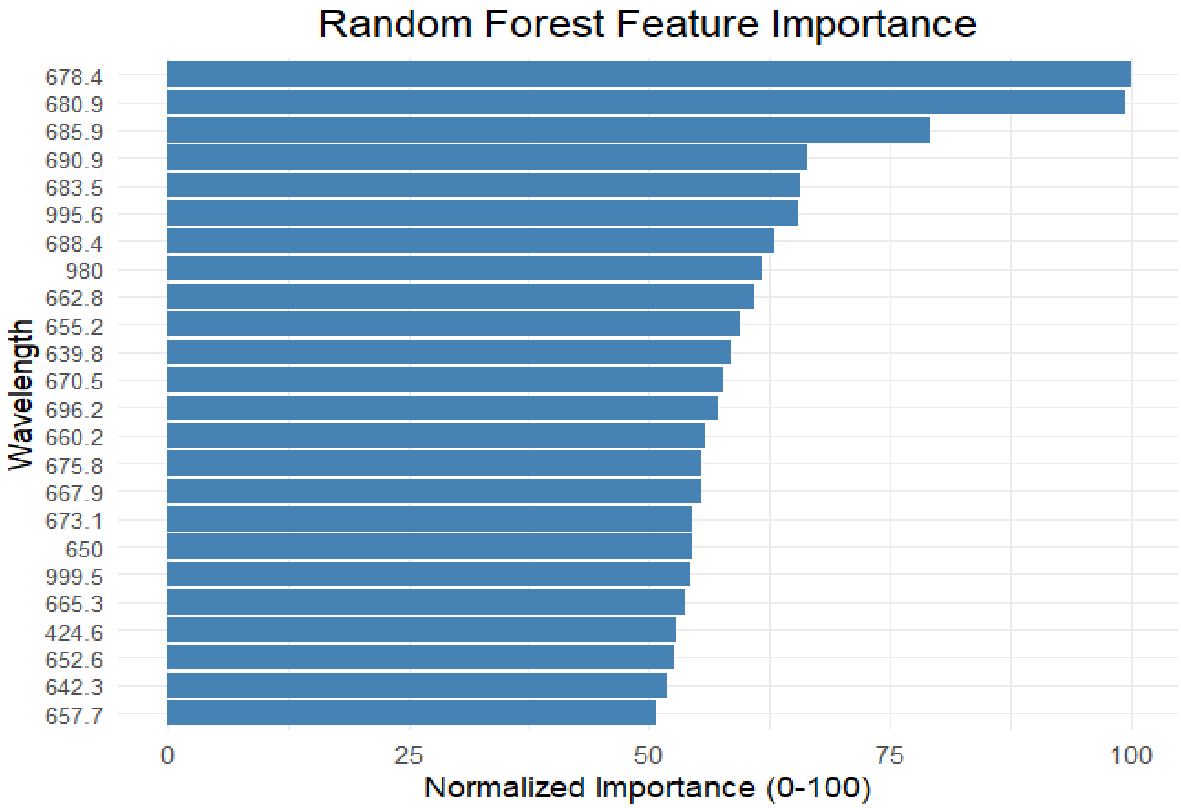

Figure APP 10: RF feature importance for DESIS Model B (Only significant bands), Only bands with at least 50% contribution were plotted.